



## Simplified chaotic oscillators with two-dimensional offset boosting

Wangyu Liu<sup>1</sup>, Chunbiao Li<sup>2,1,a</sup>, Yikai Gao<sup>1</sup>, Xin Zhang<sup>1</sup>, Yuanxiao Xu<sup>3</sup>, Jitong Xu<sup>4</sup>

<sup>1</sup> School of Electronics and Information Engineering, Nanjing University of Information Science and Technology, Nanjing 210044, China

<sup>2</sup> School of Artificial Intelligence, Nanjing University of Information Science and Technology, Nanjing 210044, China

<sup>3</sup> Digital City Intelligence Research Institute, China Information Consulting and Designing Institute CO., LTD., Nanjing 210019, China

<sup>4</sup> School of Integrated Circuits, Nanjing University of Information Science and Technology, Nanjing 210044, China

Received: 15 March 2024 / Accepted: 24 June 2024

© The Author(s), under exclusive licence to Società Italiana di Fisica and Springer-Verlag GmbH Germany, part of Springer Nature 2024

**Abstract** Chaotic systems have found widespread applications across numerous fields. The ability to obtain offset boosting independently in two dimensions within a chaotic system can meet the demands of multi-signal conditioning. In this paper, a simplified circuit is used to show the two-dimensional offset boosting for chaos based on the inherent characteristics of a multiplier. The simplified circuit structure decreases the complexity of the circuit, making chaos generation and control more easier, which has a lower cost than the traditional circuits based on those elements of summing and integrating. Finally, we implemented this chaotic system based on the platform of Field-Programmable Analogue Array (FPA) and observed the chaotic attractors on oscilloscope. The candidate of chaotic oscillator with two-dimensional offset boosting expands the perspective of chaotic signal conditioning and is beneficial for chaos-related applications.

### 1 Introduction

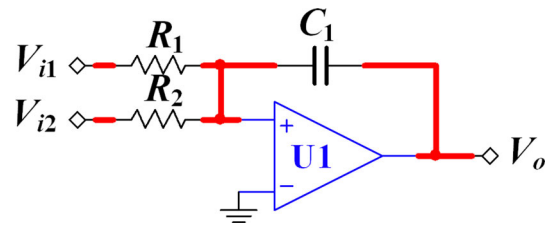
Chaos, a complex nonlinear phenomenon, is ubiquitous in physics, engineering, and other scientific disciplines [1–3]. Owing to its pseudo-randomness and sensitivity to initial conditions, chaos plays a pivotal role in various engineering applications, including secure communication [4, 5], image encryption [6–8], neuroscience [9–11], and signal denoising [12]. Offset boosting is of great significance in the research of chaotic radar systems [13–15]. Recent studies have revealed that non-bifurcation parameters in chaotic systems can facilitate more convenient amplitude adjustment and offset enhancement of signals [16–18]. Concurrently, with continuous in-depth investigations, independent offset boosting controllers have exhibited substantial potential in chaotic system applications [19–22].

This paper implements three two-dimensional offset boosting chaotic systems proposed in [22] by employing an integrated summing circuit based on operational amplifiers as the computing unit and classical chaotic circuit techniques for other nonlinear devices [23]. The influence of system constants on the offset-boosting chaos attractor is verified through simulations conducted using Multisim software. The findings not only contribute to the advancement of chaotic theory but also provide new avenues for the application of chaotic signals in radar, communication, and other domains, thereby contributing to the advancement of the field.

Furthermore, the nonlinear terms in chaotic systems present significant challenges in the implementation of chaotic circuits, which are typically realized through analog circuits [19, 24–26] or digital circuits [27–29]. The nonlinear nature of chaotic systems necessitates the design of intricate circuits, which frequently results in complex implementations. However, recent developments have focused on reducing the complexity of chaotic circuits while retaining their essential characteristics [30]. Wu et al. [31] have outlined a simplification method for variable-boostable chaotic systems based on the output characteristics of AD633. The objective of this study is to develop simplified versions of the classical circuits discussed earlier. Subsequently, the circuit principles will be utilized to enable offset boosting in these simplified chaotic circuits, thereby enhancing their practical applications and facilitating further research in this domain.

Due to the inherent limitations of digital chaotic systems in terms of precision, it is necessary to utilize analog circuit for the implementation of chaotic systems. In recent years, there has been a growing interest in Field Programmable Analog Arrays in the field of analog circuit design, due to their programmability and reconfigurability. In the implementation of chaotic systems, FPA play a fundamental role. The programmability of FPA enables designers to adapt circuit structures and parameters to specific requirements, thus facilitating the development of diverse chaotic systems. Furthermore, the utilization of FPA in analog circuitry can address the finite precision issues inherent in digital chaotic systems, thereby providing higher signal accuracy and stability.

<sup>a</sup>e-mails: goontry@126.com; chunbiaolee@nuist.edu.cn (corresponding author)

**Fig. 1** Summing integral circuit

An increasing number of scholars are employing FPAAs to construct chaotic systems. For instance, Li utilized FPAAs to construct infinitely many attractors [32]. The two-dimensional biased system discussed in this paper can also be implemented using FPAAs.

The rest of this paper is organized as follows: In Sect. 2, the classical circuits of three kinds of systems are given. In Sect. 3, the realization of the two-dimensional offset boosting of the system equation is given, and the influence of the constant term on the chaotic attractor is analyzed. In Sect. 4, simplified circuit realization of three kinds of system equations is given, and a method to realize the offset boosting in the simplified circuit is proposed and the offset boosting is verified. In Sect. 5, we will present the FPAAs implementation results of the two-dimensional offset boosting system under specific conditions. In the last section, summary and discussion are given.

## 2 Classical circuit realization

### 2.1 Offset boostable chaotic system with synchronous common control

In reference [21], Let  $(x, y, z) \rightarrow (x, -y, -z)$ , and then introducing two constants  $d_1$  and  $d_2$ , the VB8 system [21] turns out to be:

$$\begin{cases} \dot{x} = 1 - az, \\ \dot{y} = -bz^2 - y + d_2, \\ \dot{z} = x - y + d_1. \end{cases} \quad (1)$$

When  $a = 3.9$ ,  $b = 3.5$ , and the initial condition is  $[-1, 0, 0]$ , system (1) presents a chaotic state. Through multiple iterative calculations, the Lyapunov exponents of system (1) are  $(0.522, 0, -1.0523)$ , and the Kaplan-Yorke dimension is 2.0497. In terms of circuit implementation, the X-dimension of the system (1) can be transformed to obtain the corresponding X-dimension circuit representation

$$\dot{V}_o = -\frac{1}{R_1 C_1} V_{i1} - \frac{1}{R_2 C_1} V_{i2} \quad (2)$$

In order to facilitate the circuit realization of the system, the Eq. (2) is further simplified, and the time  $t$  is integrated on both sides at the same time.

$$V_o = -\frac{1}{R_1 C_1} \int V_{i1} dt - \frac{1}{R_2 C_1} \int V_{i2} dt \quad (3)$$

The summing integrated circuit corresponding to Eq. (3) is shown in Fig. 1. Based on this principle, the same change operation can be carried out for other dimensions of the equation of system (1). The analogue circuit for system (1) are shown in Fig. 2.

In the figure above, the multiplier is used to realize the quadratic term  $-z^2$ , and then the DC power supply  $V_1$ ,  $V_2$  and  $V_3$  are respectively used to realize the constant term in the system, the addition and subtraction of variables are realized in combination with the superposition theorem, and the inverse phase proportional operation circuit is used to complete the inverse phase operation of variables. Here, The AD633JN is adopted for the multiplier, and the LM741CN is adopted for the operational amplifier. The corresponding circuit equation of system (1) is as follows:

$$\begin{cases} \dot{x} = \frac{V_3}{R_1 C_1} - \frac{z}{R_2 C_1}, \\ \dot{y} = -\frac{z^2}{R_3 C_2} - \frac{y}{R_4 C_2} - \frac{V_2}{R_5 C_2}, \\ \dot{z} = \frac{x}{R_7 C_3} - \frac{y}{R_6 C_3} - \frac{V_1}{R_8 C_3}. \end{cases} \quad (4)$$

According to reference [21], when  $a = 3.9$  and  $b = 3.5$ , system (1) presents chaotic state under initial condition  $IC = [-1, 0, 0]$ , circuit parameters are set here:  $R_1 = R_4 = R_5 = R_6 = R_7 = 10 \text{ k}\Omega$ ,  $R_9 = R_{10} = 20 \text{ k}\Omega$ ,  $R_3 = 280 \Omega$ ,  $R_2 = 2.4 \text{ k}\Omega$ , all capacitors are  $10 \text{ nF}$ ,  $V_3 = 1 \text{ V}$ ,  $V_1 = V_2 = 0 \text{ V}$ ,  $\text{VCC} = 15 \text{ V}$ ,  $\text{VEE} = -15 \text{ V}$ . Comparing Figs. 3 and 4, it is found that the circuit output is consistent with the numerical simulation results.

**Fig. 2** Classical circuits of system (1)

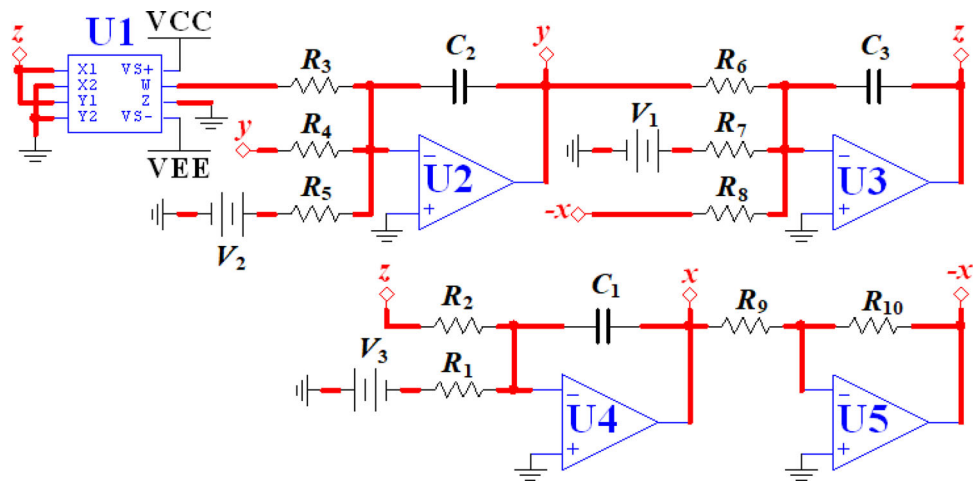
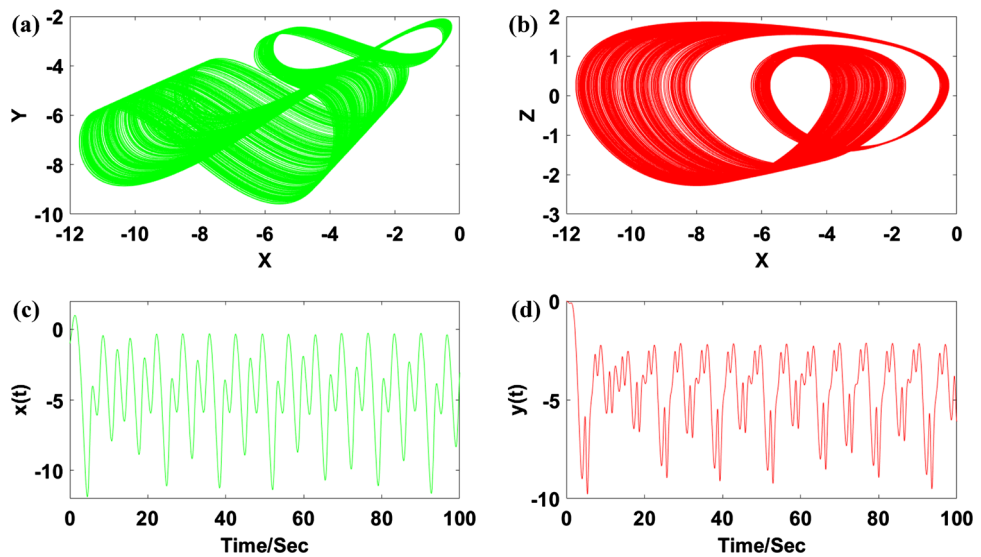


**Fig. 3** Chaotic oscillation in system (1) with  $a = 3.9$ ,  $b = 3.5$  and IC =  $(-1, 0, 0)$ : **a**  $x$ - $y$  plane, **b**  $x$ - $z$  plane, **c** chaotic signal  $x(t)$ , **d** chaotic signal  $y(t)$



## 2.2 Offset boostable chaotic system with synchronous reverse control

Additional linear feedback is added to VB7 in reference [21], substitution  $y \rightarrow -y$  is adopted and constant  $d_1$  is introduced, along with  $d_2$  shown in system (5). For system (5), when we set  $a = 0.55$ ,  $b = 0.4$  and the initial condition is  $[1, -1, -1]$ , it presents a chaotic state, the Lyapunov exponents are  $(0.0506, 0, -0.601)$ , and the Kaplan-Yorke dimension is 2.0843.

$$\begin{cases} \dot{x} = z^2 + y + d_2, \\ \dot{y} = -bz, \\ \dot{z} = -az + x + y + d_1. \end{cases} \quad (5)$$

By the same way, a classical circuit can be constructed, as shown in Fig. 5.

By similar analysis, the circuit equation can be obtained as follows:

$$\begin{cases} \dot{x} = \frac{z^2}{R_1 C_1} + \frac{y}{R_2 C_1} - \frac{V_2}{R_{10} C_1}, \\ \dot{y} = -\frac{z}{R_3 C_2}, \\ \dot{z} = -\frac{z}{R_4 C_3} + \frac{x}{R_5 C_3} + \frac{y}{R_6 C_3} - \frac{V_1}{R_7 C_3}. \end{cases} \quad (6)$$

When  $a = 0.55$ ,  $b = 0.4$ , system (5) outputs chaotic signal under the initial condition  $[1, -1, -1]$ . Here the circuit parameters are set as follows:  $R_2 = R_5 = R_6 = R_7 = R_{10} = 10 \text{ k}\Omega$ ,  $R_8 = R_9 = R_{11} = R_{12} = 20 \text{ k}\Omega$ ,  $R_1 = 1 \text{ k}\Omega$ ,  $R_3 = 25 \text{ k}\Omega$ ,  $R_4 = 18 \text{ k}\Omega$ , all

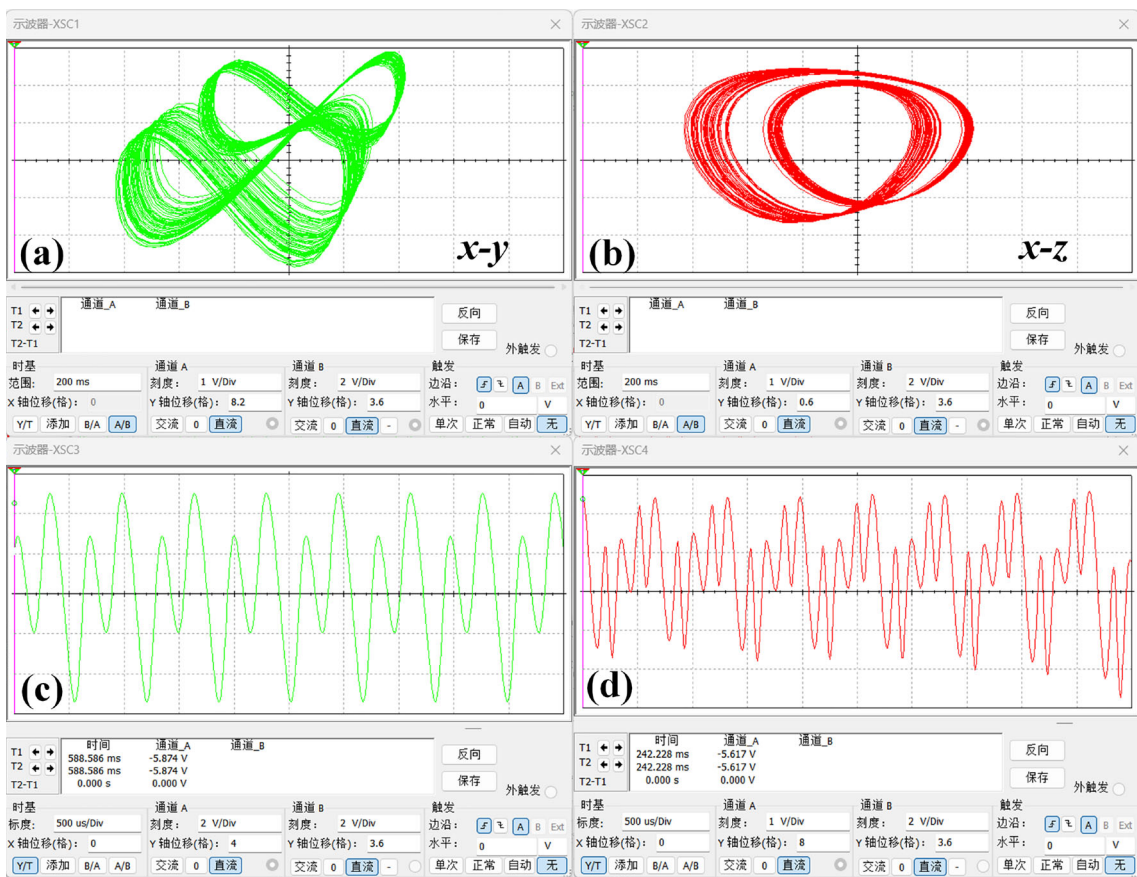
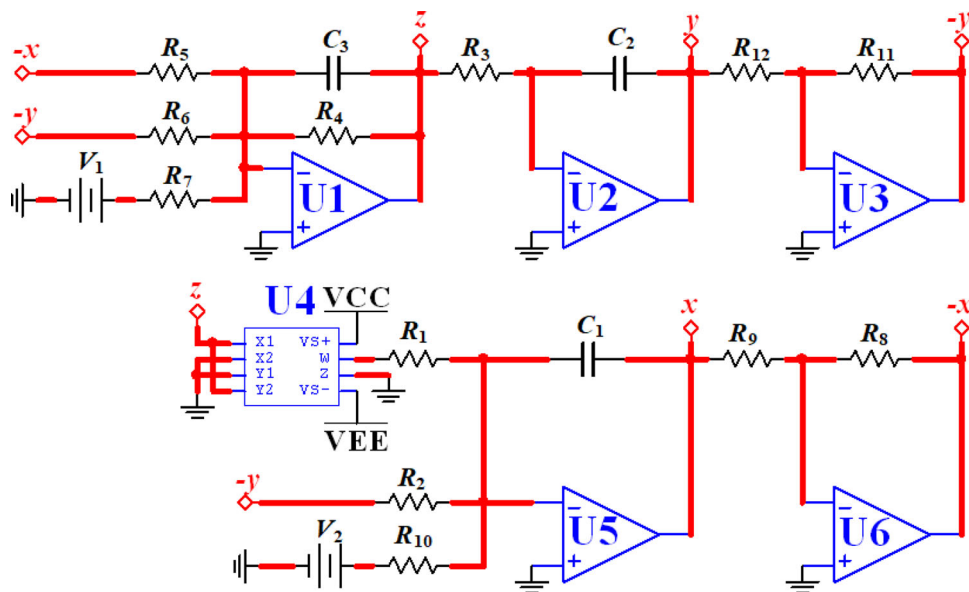


**Fig. 4** Circuit output diagram of system (1): **a**  $x$ - $y$  plane, **b**  $x$ - $z$  plane, **c** chaotic signal  $x(t)$ , **d** chaotic signal  $y(t)$

**Fig. 5** Classic circuit of system (5)



capacitors are  $10 \text{ nF}$ ,  $V_1 = V_2 = 0 \text{ V}$ ,  $\text{VCC} = 15 \text{ V}$ ,  $\text{VEE} = -15 \text{ V}$ . The phase track diagram and waveform diagram generated by the circuit are shown in Fig. 6 and are consistent with the MATLAB numerical simulation results in Fig. 7.

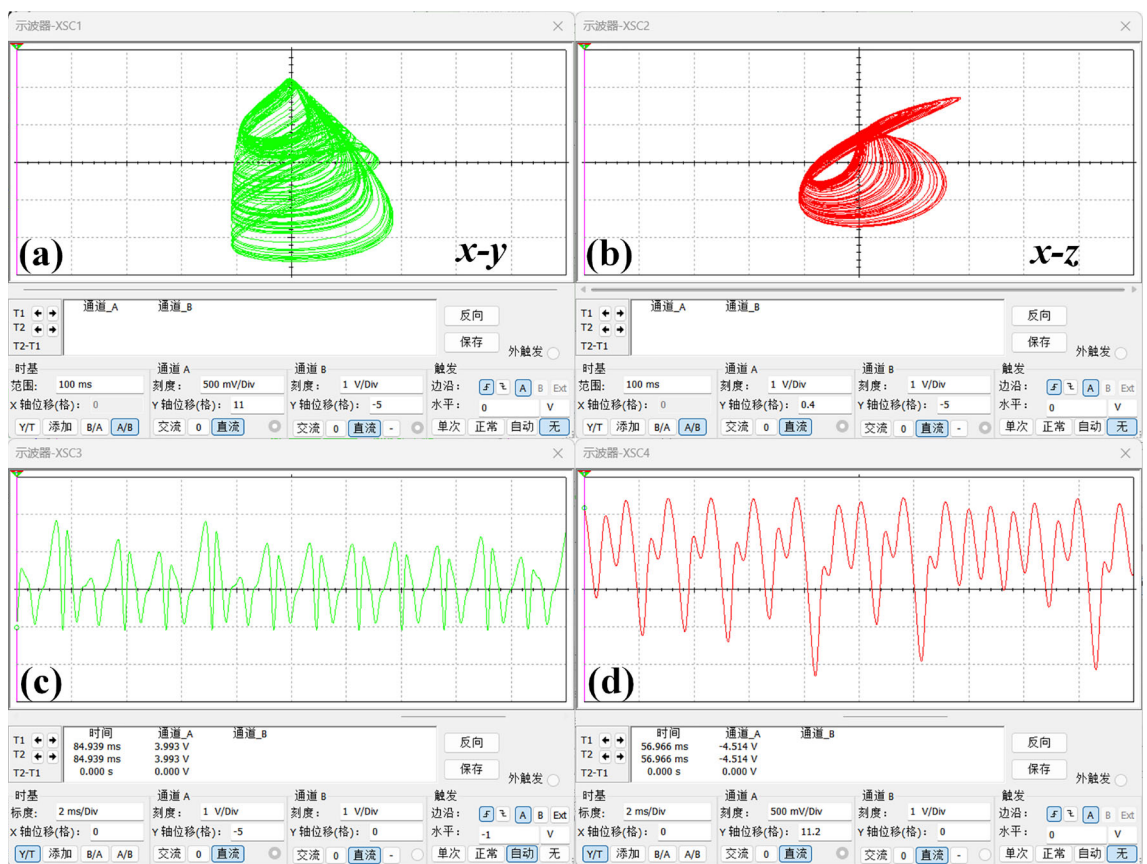


**Fig. 6** Circuit output diagram of system (5): **a**  $x$ - $y$  plane, **b**  $x$ - $z$  plane, **c** chaotic signal  $x(t)$ , **d** chaotic signal  $y(t)$

**Fig. 7** Chaotic oscillation in system (5) with  $a = 0.55$ ,  $b = 0.4$  and IC =  $(1, -1, -1)$ : **a**  $x$ - $y$  plane, **b**  $x$ - $z$  plane, **c** chaotic signal  $x(t)$ , **d** chaotic signal  $y(t)$

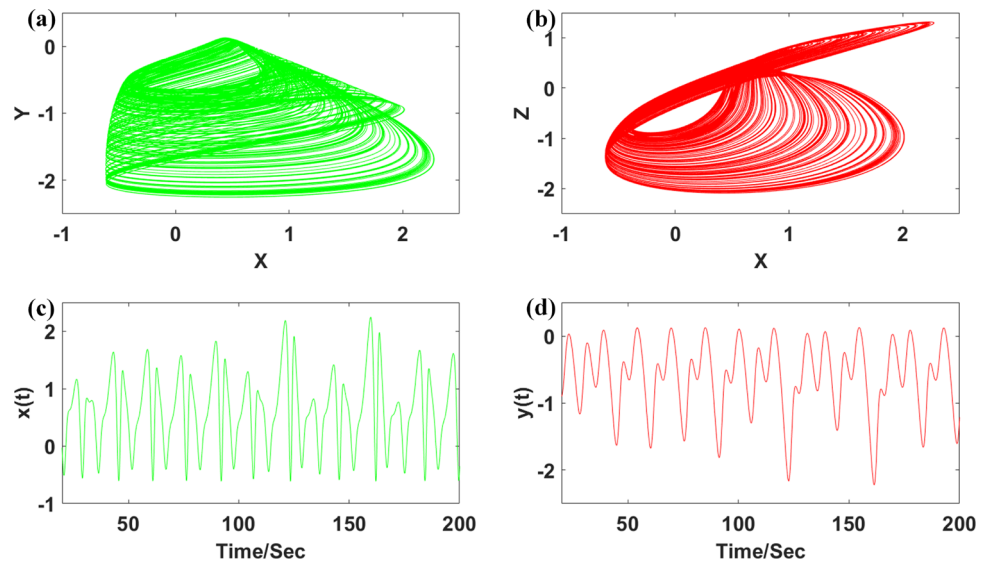
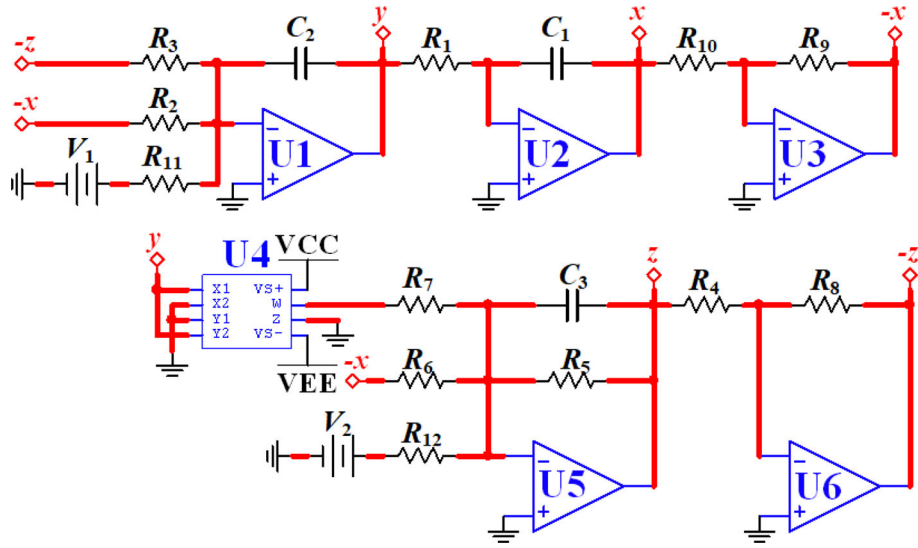


**Fig. 8** Classical circuit of system (7)



### 2.3 Offset boostable chaotic system with coexisting common and reverse control

Reference [20] introduces constant  $d_1$  to Sprott I system,  $d_2$  gets system (7), in which two constants  $d_1, d_2$  can realize independent offset boosting. For system (7), when we set  $a = 0.2$  and the initial condition is  $[0, 0.3, 0]$ , it presents a chaotic state, the Lyapunov exponents is  $(0.012, 0, -1.012)$ , and the Kaplan–Yorke dimension is 2.0114.

$$\begin{cases} \dot{x} = -ay, \\ \dot{y} = x + z + d_1, \\ \dot{z} = x - z + y^2 + d_2. \end{cases} \quad (7)$$

In the same way, a classical circuit can also be constructed, as shown in Fig. 8:

Applying the superposition theorem, the circuit equation is obtained as follows:

$$\begin{cases} \dot{x} = -\frac{y}{R_1 C_1}, \\ \dot{y} = \frac{x}{R_2 C_2} + \frac{z}{R_3 C_2} - \frac{V_1}{R_{11} C_2}, \\ \dot{z} = \frac{x}{R_5 C_3} - \frac{z}{R_6 C_3} + \frac{y^2}{R_7 C_3} - \frac{V_2}{R_{12} C_3}. \end{cases} \quad (8)$$

Reference [20] points out that when  $a = 0.2$ , system (7) appears chaotic state under the initial condition  $[0, 0.3, 0]$ . To realize system (7), the circuit parameters of system (8) can be set as follows:  $R_2 = R_3 = R_5 = R_6 = R_{11} = R_{12} = 10 \text{ k}\Omega$ ,  $R_4 = R_8 = R_9 = R_{10} = 20 \text{ k}\Omega$ ,  $R_7 = 1 \text{ k}\Omega$ ,  $R_1 = 38 \text{ k}\Omega$ , capacitors are all set to  $10 \text{ nF}$ ,  $V_1 = V_2 = 0 \text{ V}$ ,  $\text{VCC} = 15 \text{ V}$ ,  $\text{VEE} = -15 \text{ V}$ . The phase track diagram produced by the circuit is shown in Fig. 9, which is obviously consistent with the numerical simulation results in Fig. 10.

## 3 Offset boosting by two independent constants

### 3.1 Offset boosting analysis

Here the two parameters  $d_1$  and  $d_2$  in system (1) do not affect the dynamical behavior of the system, where the parameter  $d_1$  provides direct offset boosting with the variable  $x$ , while the parameter  $d_2$  gives synchronous common offset control to the variables  $x$  and  $y$ .

$$\begin{cases} \dot{x} = 1 - az, \\ \dot{y} = -bz^2 - y, \\ \dot{z} = x - y. \end{cases} \quad (9)$$

Take the substitutions of  $x \rightarrow d_2 - d_1$ ,  $y \rightarrow y + d_2$ , system (1) returns to be an original one like the equation of (9) without parameters  $d_1$  and  $d_2$ , indicating that those parameters do not revise the dynamics but only driving corresponding offset boosting of variables  $x$ , and  $y$ .

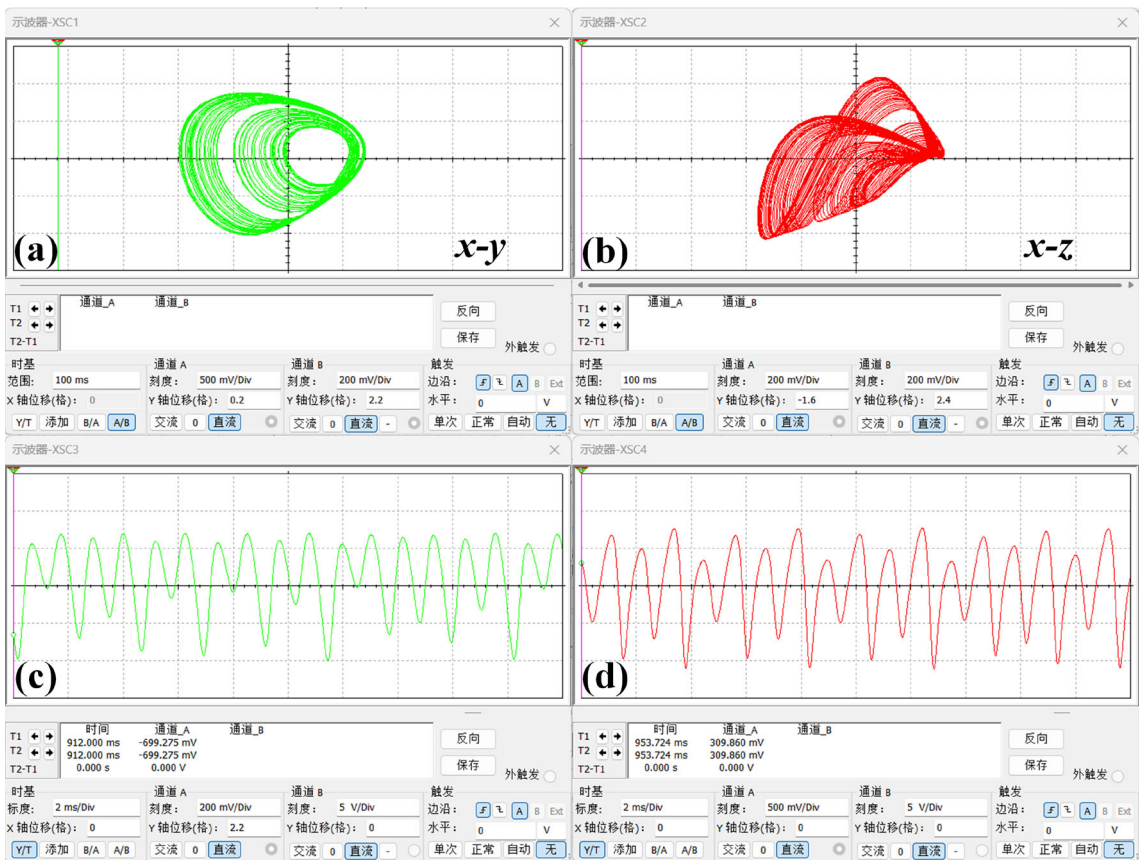
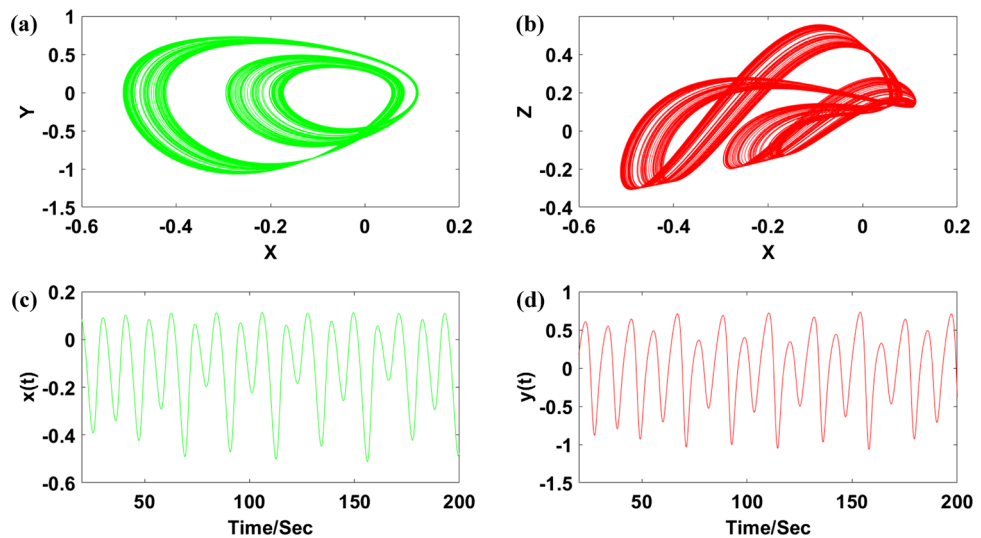


**Fig. 9** Circuit output diagram of system (7): **a**  $x$ - $y$  plane, **b**  $x$ - $z$  plane, **c** chaotic signal  $x(t)$ , **d** chaotic signal  $y(t)$

**Fig. 10** Chaotic oscillation in system (7) with  $a = 0.2$  and IC =  $(0, 0.3, 0)$ : **a**  $x$ - $y$  plane, **b**  $x$ - $z$  plane, **c** chaotic signal  $x(t)$ , **d** chaotic signal  $y(t)$



For system (1), the Lyapunov exponents shown in Fig. 11 do not shake when we vary the offset parameters  $d_1$  and  $d_2$ , and it can be seen from the bifurcation diagram that parameters  $d_1$  and  $d_2$  have opposite effects on variable  $x$ . Meanwhile, as shown in Fig. 12, when the offset parameter  $d_1$  varies in  $[-10, 10]$  and  $d_2$  remains zero, the value of variable  $x$  decreases, while the value of the variable  $y$  and  $z$  do not change. When the offset parameter  $d_2$  varies in  $[-10, 10]$  and  $d_1$  remains zero, the value of variable  $x$  and  $y$  increase synchronously, while the value of the variable  $z$  do not change. These indicate that the parameter  $d_1$  can control the value of  $x$  in the reverse direction, and  $d_2$  can control the values of  $x$  and  $y$  in the positive direction at the same time.

**Fig. 11** Dynamical behaviors of system (1) with  $a = 3.9, b = 3.5$ : **a** Lyapunov exponents when  $d_2 = 0, d_1 \in [-10, 10]$ , **b** Bifurcation diagram when  $d_2 = 0, d_1 \in [-10, 10]$ , **c** Lyapunov exponents when  $d_1 = 0, d_2 \in [-10, 10]$ , **d** Bifurcation diagram when  $d_1 = 0, d_2 \in [-10, 10]$

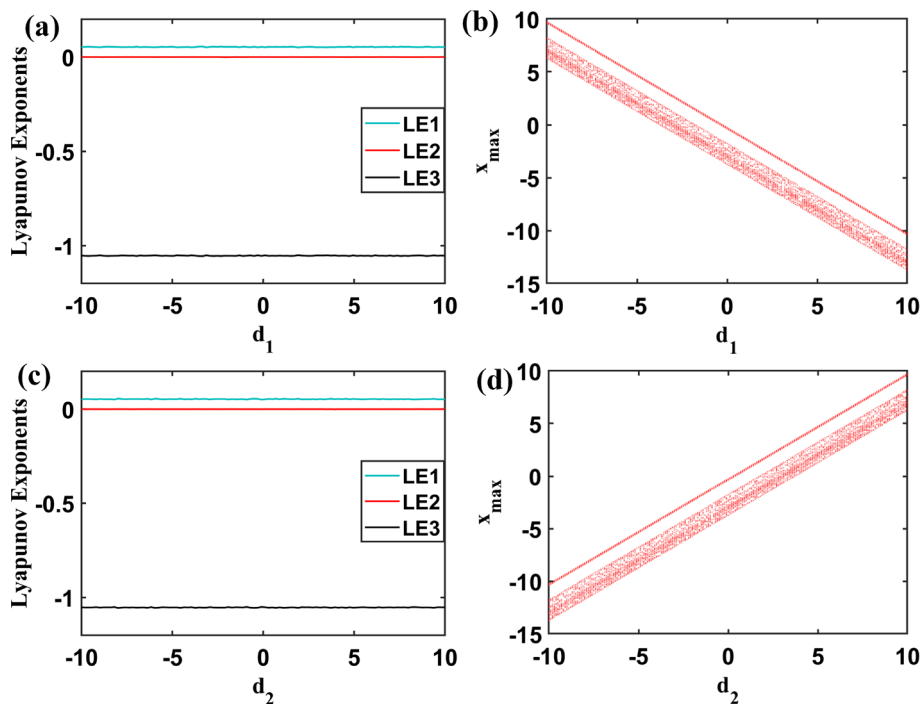


**Fig. 12** The average value of the variables in system (1) with  $a = 3.9, b = 3.5$ : **a**  $d_2 = 0, d_1 \in [-10, 10]$ , **b**  $d_1 = 0, d_2 \in [-10, 10]$

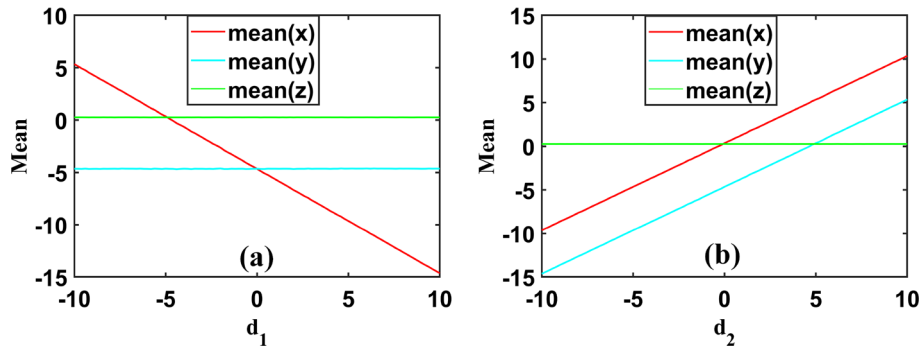
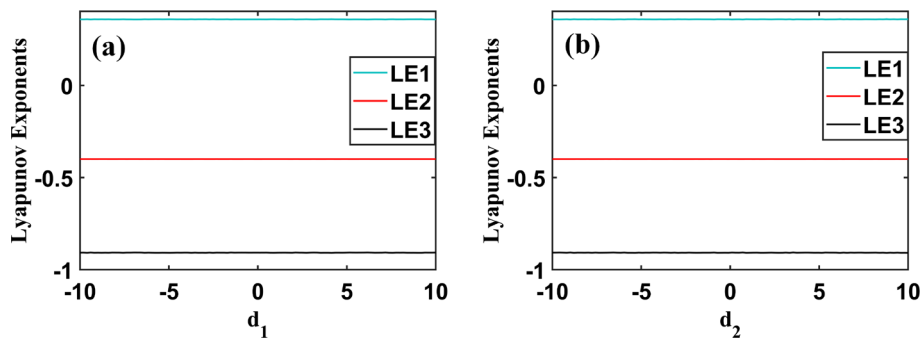


**Fig. 13** Dynamical behaviors of system (5) with  $a = 0.55, b = 0.4$ : **a** Lyapunov exponents when  $d_2 = 0, d_1 \in [-10, 10]$ , **b** Lyapunov exponents when  $d_1 = 0, d_2 \in [-10, 10]$



In fact, for the other two cases like systems (5) and system (7), the introduction of the parameters  $d_1$  and  $d_2$  similarly do not change the dynamics of the systems, the inherent principle hidden in this situation is the same as proved above. However, the patterns of offset boosting are different due to the system structure.

As shown in Fig. 13, when the offset parameters  $d_1$  and  $d_2$  are changed in system (5), Lyapunov exponents still do not change and do not produce other bifurcation cases. As shown in Fig. 14, when we change  $d_1$  from -10 to 10, the value of variable  $x$  decreases, while the value of variable  $y$  and  $z$  do not change. When the offset parameter  $d_2$  varies in  $[-10, 10]$  and  $d_1$  remains zero, the value of variable  $x$  increases and the value of variable  $y$  decreases. The effect of  $d_2$  in system (5) and  $d_2$  in system (1) is similar, and two values can be controlled at the same time. The difference is that  $d_2$  in system (5) can realize the reverse control of two values.

**Fig. 14** The average value of the variables in system (5) with  $a = 0.55$ ,  $b = 0.4$ : **a** The average value of the variables when  $d_2 = 0$ ,  $d_1 \in [-10, 10]$ , **b** The average value of the variables when  $d_1 = 0$ ,  $d_2 \in [-10, 10]$

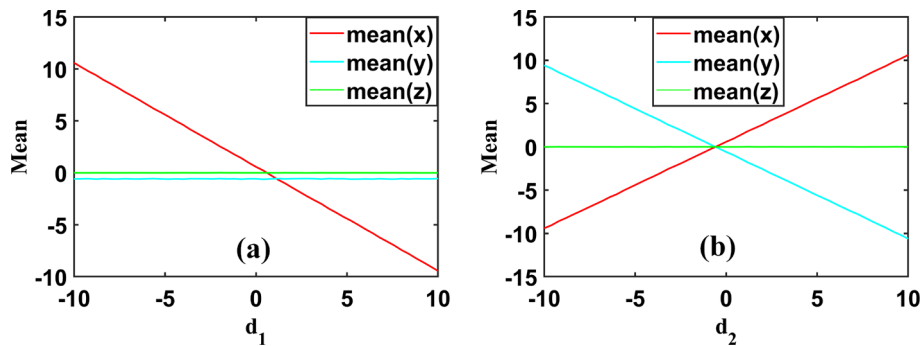


**Fig. 15** Dynamical behaviors of system (7) with  $a = -0.2$ : **a** Lyapunov exponents when  $d_2 = 0$ ,  $d_1 \in [-10, 10]$ , **b** Lyapunov exponents when  $d_1 = 0$ ,  $d_2 \in [-10, 10]$

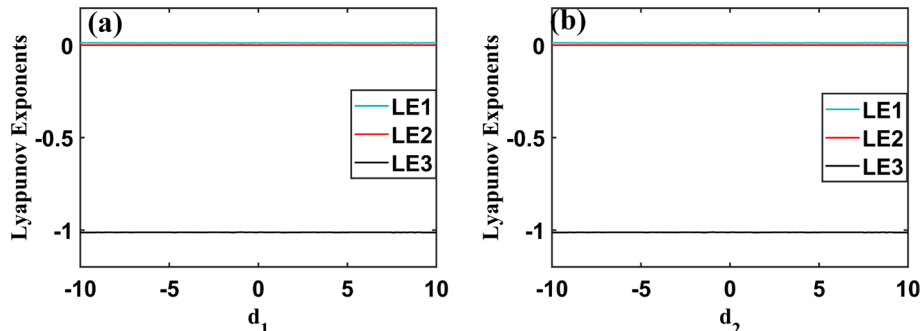
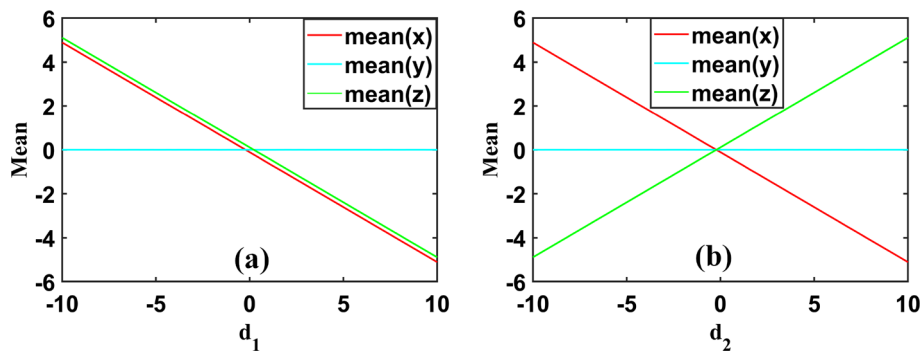


**Fig. 16** The average value of the variables in system (7) with  $a = 0.2$ : **a**  $d_2 = 0$ ,  $d_1 \in [-10, 10]$ , **b**  $d_1 = 0$ ,  $d_2 \in [-10, 10]$



The Lyapunov exponents of system (7) are shown in Fig. 15. Figure 16 give the average value of the variables of system (7). We can see that the two offset parameters  $d_1$  and  $d_2$  in system (7) are different from the previous two systems, and both  $d_1$  and  $d_2$  can control the two values at the same time. When the offset parameter  $d_1$  varies in  $[-10, 10]$  and  $d_2$  remains zero, the value of variable  $x$  and  $z$  decrease. When the offset parameter  $d_2$  varies in  $[-10, 10]$  and  $d_1$  remains zero, the value of variable  $x$  decreases and the value of variable  $z$  increases.

### 3.2 Offset boosting under synchronous common control

The principle of circuit offset boosting is to use the combination of DC signal and AC signal, so that the output signal can be operated in an effective range. The stable DC voltage can effectively enable the circuit to operate at the appropriate operating point, thereby achieving the required function. In the classical circuit above, the method of combining DC power supply and resistance in series in the summing integral circuit is used to realize the independent constants  $d_1$  and  $d_2$  that provide the offset boosting in the equation. Based on this, the effect of the constant on the offset can be analyzed by changing the voltage value of the DC power supply and the initial condition (IC) of the capacitor, and then observing the change of the chaotic attractor or variable waveform. In reference [21], the initial condition of system (1) is modified to  $[-1 - d_1 + d_2, d_2, 0]$ , and the 3D offset boosting of the attractor is shown in the  $x$ - $y$  and  $x$ - $z$  planes. We change the value of  $V_1$  in the circuit Eq. (4) and the initial value of the capacitance, keeping  $V_2 = 0$  V, as shown in Fig. 17. When  $d_1$  is reduced from 0 to  $-5$ , the chaotic attractor moves in the positive direction of  $x$  while no offset occurs in other dimensions, indicating that the negative constant  $d_1$  causes the attractor to move in the positive direction of  $x$ .

Change the value of  $V_2$  in the circuit Eq. (4) and the initial value of the capacitance, keeping  $V_1 = 0$  V, as shown in Fig. 18. When  $d_2$  increases from 0 to 5, the chaotic attractor moves in the  $x$ ,  $y$  positive direction, while it does not move in the  $z$  direction, indicating that the normal number  $d_2$  causes the attractor to move in the  $x$ ,  $y$  positive direction.

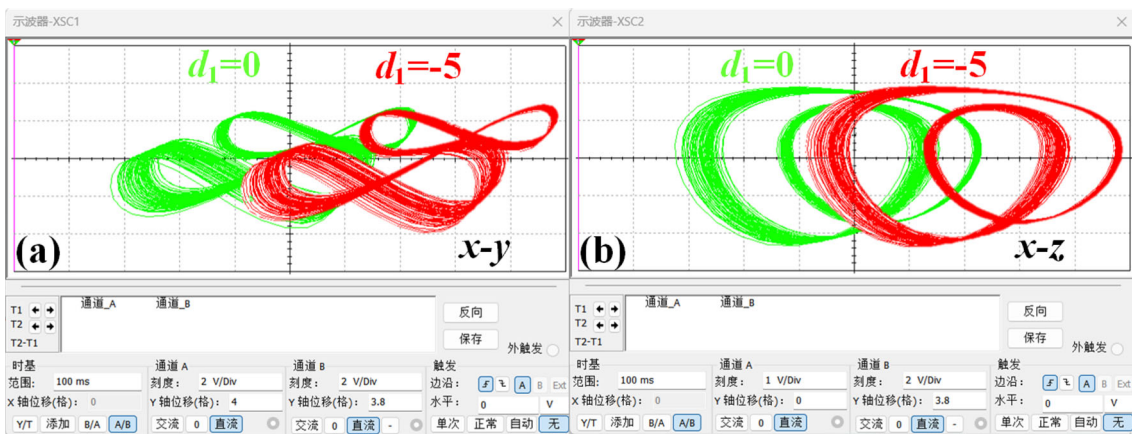


**Fig. 17** Single offset boosting control in system (1) with  $d_2 = 0$ : **a**  $x-y$ , **b**  $x-z$ . Here  $d_1 = 0$ , IC  $= (-1, 0, 0)$  is green,  $d_1 = -5$ , IC  $= (4, 0, 0)$  is red

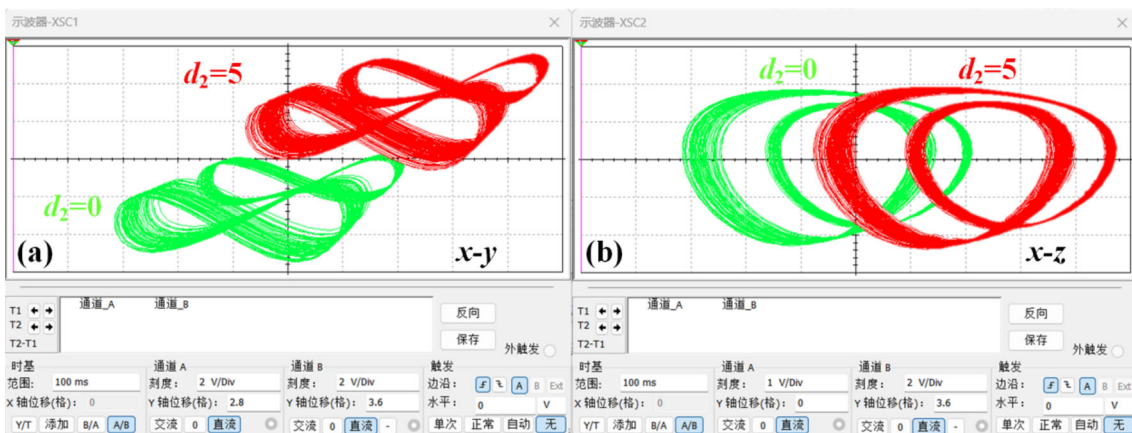


**Fig. 18** Common offset boosting control in system (1) with  $d_1 = 0$ : **a**  $x-y$ , **b**  $x-z$ . Here  $d_1 = 0$ , IC  $= (-1, 0, 0)$  is green,  $d_2 = 5$ , IC  $= (4, 5, 0)$  is red

### 3.3 Offset boosting under synchronous reverse control

For the offset boosting of system (5), the same operation is used as for the circuit equation of system (4), adjusting the initial conditions of  $V_1$ ,  $V_2$  and capacitance, and observing the changes of the attractor and waveform on the oscilloscope. The initial conditions of system (5) is modified in the reference [21] as  $[-1 - d_1 + d_2, -1 - d_2, -1]$ . As shown in Fig. 19, when  $d_1$  increases from 0 to  $-5$ , the  $x$  waveform moves in the positive direction, while the  $y$  and  $z$  waveforms do not move.

Change the value of  $V_2$  in the circuit Eq. (6) and the initial value of the capacitance, keeping  $V_2 = 0$  V, as shown in Fig. 20 when  $d_2$  increases from 0 to 5, the chaotic attractor moves in the  $x$  positive direction and  $y$  negative direction; The  $x$  waveform moves up, the  $y$  waveform moves down and the  $z$  waveform does not move, indicating that the normal number  $d_2$  causes the attractor to move in the positive direction of variables  $x$  and  $y$ .

### 3.4 Offset boosting under coexisting common and reverse control

Take the same action as above for system (7) to adjust the  $V_1$ ,  $V_2$  and capacitance initial conditions in system (7). Observe the change of the attractor on the oscilloscope, as shown in Fig. 21. When  $d_1$  is reduced to  $-5$ , the chaotic attractor moves in the positive direction of  $x$ ,  $z$ .

Change the value in the circuit Eq. (7) and the initial value of the capacitance, keeping  $V_1 = 0$  V, as shown in Fig. 22. When  $d_2$  increases from 0 to 5, the  $x$  waveform moves down, the  $z$  waveform moves up, and the  $y$  waveform does not move, indicating that the normal number  $d_2$  causes the attractor to move in the  $x$  negative direction and  $z$  positive direction.

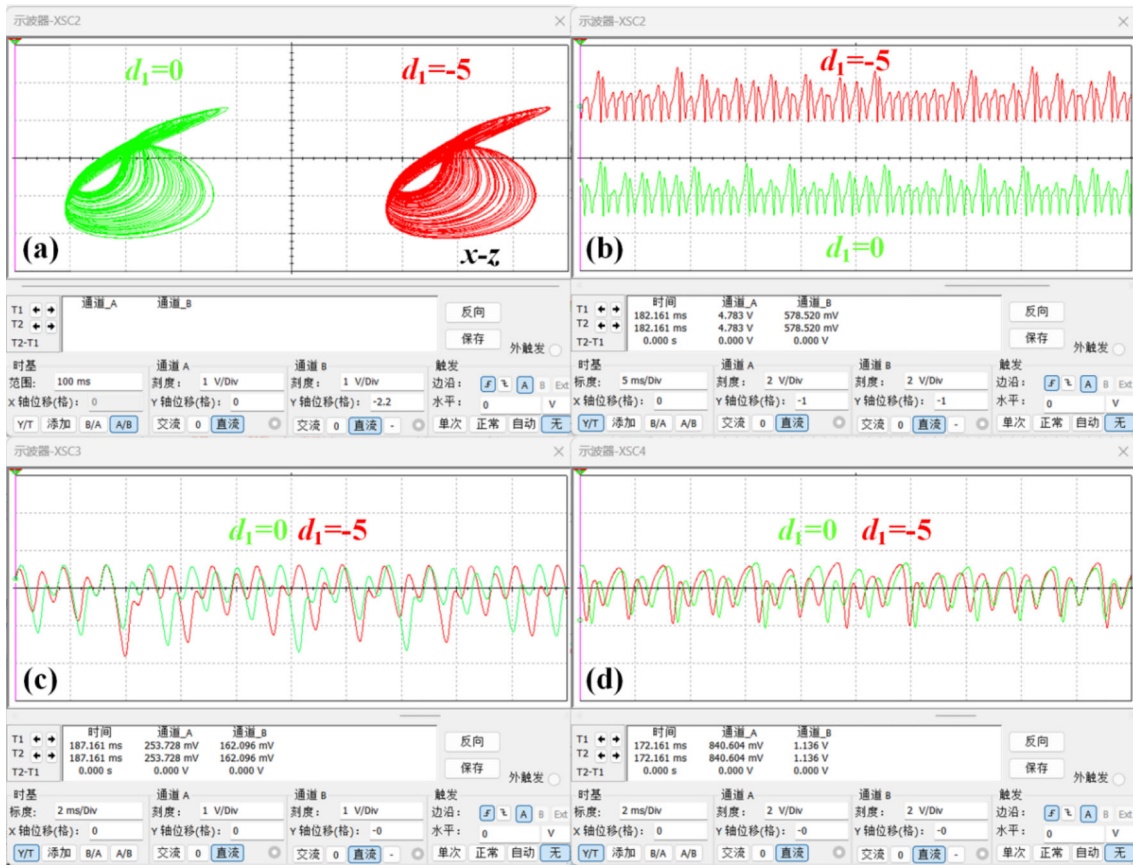


**Fig. 19** Single offset boosting in system (5) with  $d_2 = 0$ : **a**  $x$ - $y$ , **b** chaotic signal  $x(t)$ , **c** chaotic signal  $y(t)$ , **d** chaotic signal  $z(t)$ . Here  $d_1 = 0$ , IC = (1, 0, 0) is green,  $d_1 = -5$ , IC = (6, -1, 1) is red

#### 4 Simplified circuits

In reference [29], a new hybrid structure based on multiplier and resistance–capacitance coupling is proposed. It is pointed out that in the chaotic system circuit with quadratic terms, the voltage output can be converted into current output by means of external resistance of the multiplier, and flexible current output can be obtained through the configuration of the input port of the multiplier. Combined with the resistance–capacitance coupling structure, flexible differential constraints can be realized.

The circuit complexity is reduced after simplification, as shown in Table 1. The red numbers in the table indicate that the circuit constructed by another method with the same system uses more devices. Observing the table, we find that compared with the classical circuit, the simplified circuit only needs to add one or two multipliers, which can reduce the use of several op-amps and resistors, improve the multiplier, op-amps and capacitor utilization, reduce the circuit complexity and reduce the cost. At the same time, because the number of components is reduced, the simplified circuit is more suitable for constructing robust chaotic equations.

Based on the above principles, the above three systems can be simplified. To ensure that the simplified circuit is not complicated, the system equation is first simplified without introducing the constant  $d_1$ ,  $d_2$ . System (1), system (5) and system (7) without introducing the constant  $d_1$ ,  $d_2$  are described as:

$$\begin{cases} \dot{x} = 1 - az, \\ \dot{y} = -bz^2 - y, \\ \dot{z} = x - y. \end{cases} \quad (10)$$

$$\begin{cases} \dot{x} = z^2 + y, \\ \dot{y} = -bz, \\ \dot{z} = -az + x + y. \end{cases} \quad (11)$$

$$\begin{cases} \dot{x} = -ay, \\ \dot{y} = x + z, \\ \dot{z} = x - z + y^2. \end{cases} \quad (12)$$

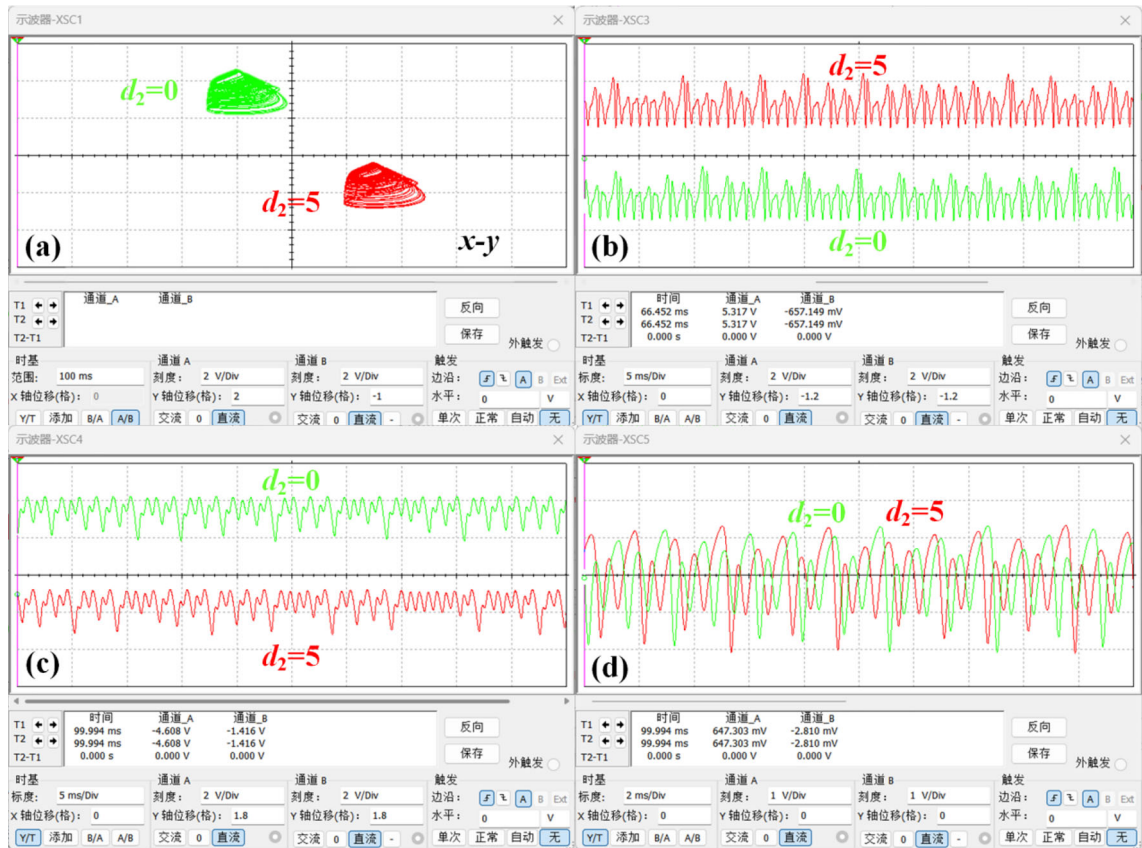


**Fig. 20** Offset boosting of reverse in system (5) with  $d_1 = 0$ : **a**  $x-y$  plane, **b** chaotic signal  $x(t)$ , **c** chaotic signal  $y(t)$ , **d** chaotic signal  $z(t)$ . Where  $d_2 = 0$ , IC = (1, 1, 1) for the green,  $d_2 = 5$ , IC = (6, 6, 1) in red

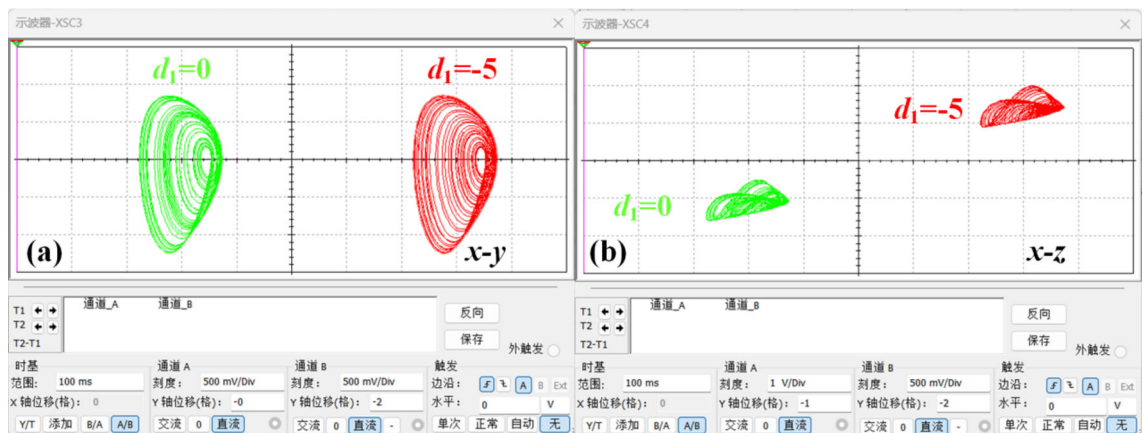


**Fig. 21** Single offset boosting control in system (7) with  $d_2 = 0$ : **a**  $x-y$ , **b**  $x-z$ . Here  $d_1 = 0$ , IC = (0, 0.3, 0) is green,  $d_1 = -5$ , IC = (2.5, 0.3, 2.5) is red

#### 4.1 Simplified circuit of system (10)

The simplified circuit of system (10) is shown in Fig. 23, in which only three multipliers and several resistors and capacitors are used, and the operational amplifier is omitted. In system (10), we use the combination of multipliers and capacitors for the equation  $\dot{x} = 1 - az$ ; For the equation  $\dot{y} = -bz^2 - y$ , we use the multiplier to construct the quadratic term  $-bz^2$ , and use the parallel coupling of resistance and capacitance to realize  $-y$ ; For the equation  $\dot{z} = x - y$ , due to the combination of the multiplier and the resistor can achieve flexible current output, we use the multiplier and the resistor in series, the DC power supply  $V_3$  compensation up to 10 times, and then connect the capacitor can easily realize the integration of  $x-y$ .

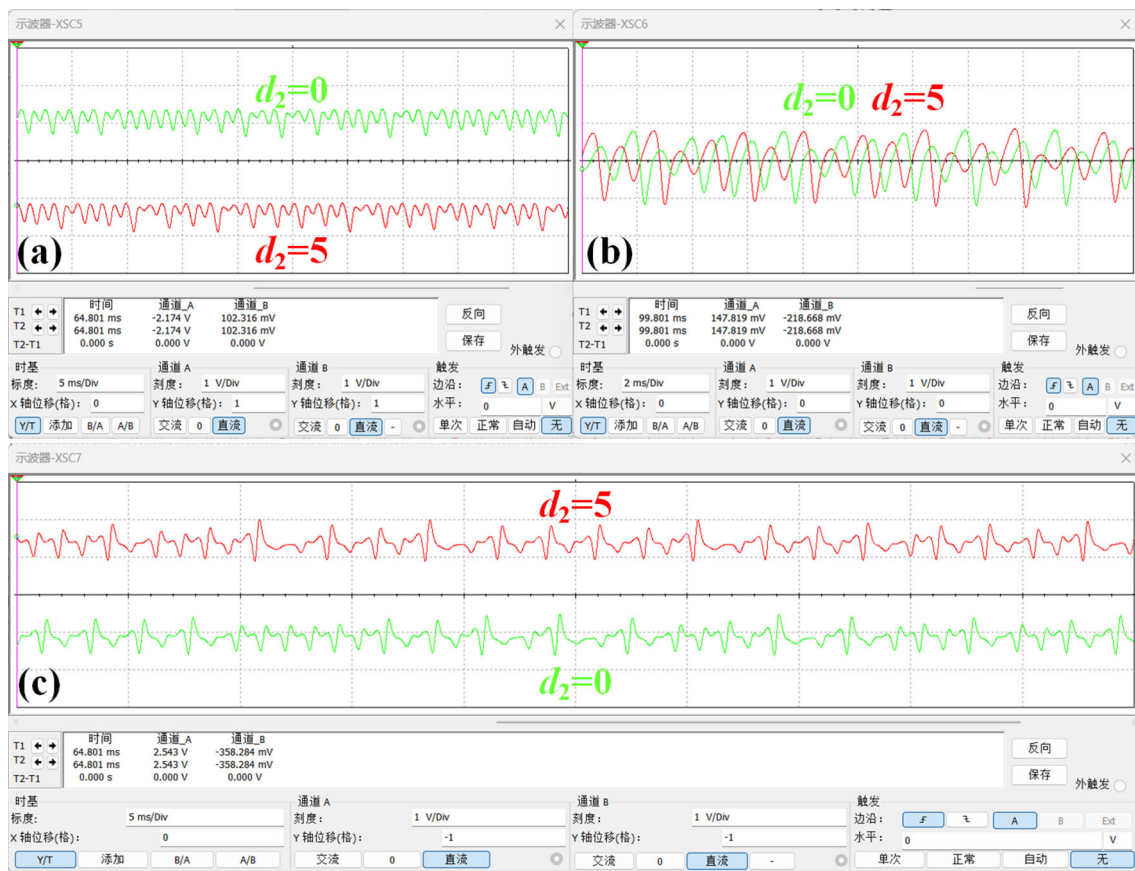


**Fig. 22** Reverse offset boosting control in system (7) with  $d_1 = 0$ : **a** chaotic signal  $x(t)$ , **b** chaotic signal  $y(t)$ , **c** chaotic signal  $z(t)$ . Here  $d_2 = 0$ , IC = (0, 0.3, 0) is green,  $d_2 = 5$ , IC = (−2.5, 0.3, 2.5) is red

**Table 1** The number of main components in the classical circuit and simplified circuit of the system

Circuits	Op-AMP	Multiplier	Resistors	Capacitance
System (1) classic circuit	4	1	10	3
System (1) simplified circuit	0	3	4	3
System (3) classic circuit	5	1	12	3
System (3) simplified circuit	3	2	7	3
System (5) classic circuit	5	1	11	3
System (5) simplified circuit	2	2	6	3

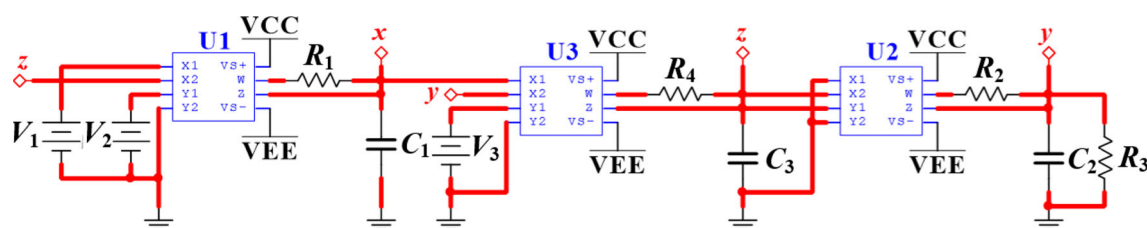


**Fig. 23** Simplified circuit of system (10)

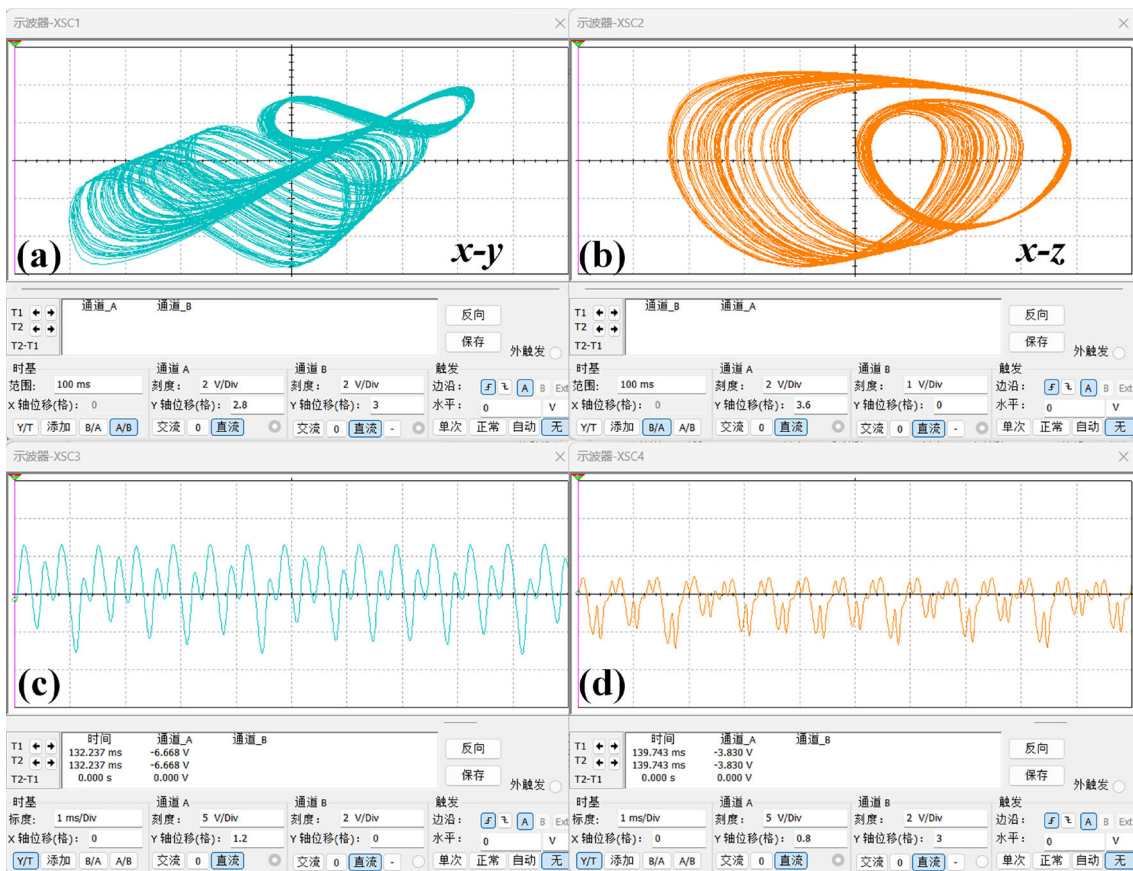


**Fig. 24** Phase track diagram and waveform diagram of simplified circuit of system (10): **a**  $x$ - $y$  plane, **b**  $x$ - $z$  plane, **c** chaotic signal  $x(t)$ , **d** chaotic signal  $y(t)$

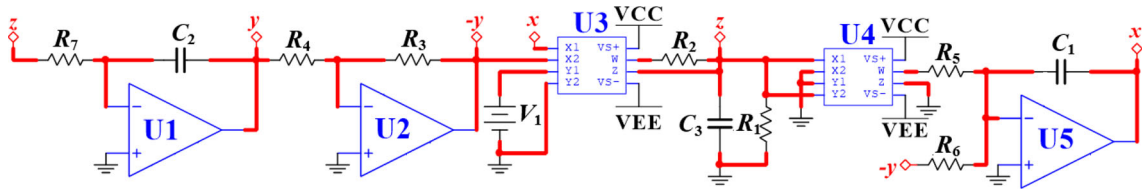
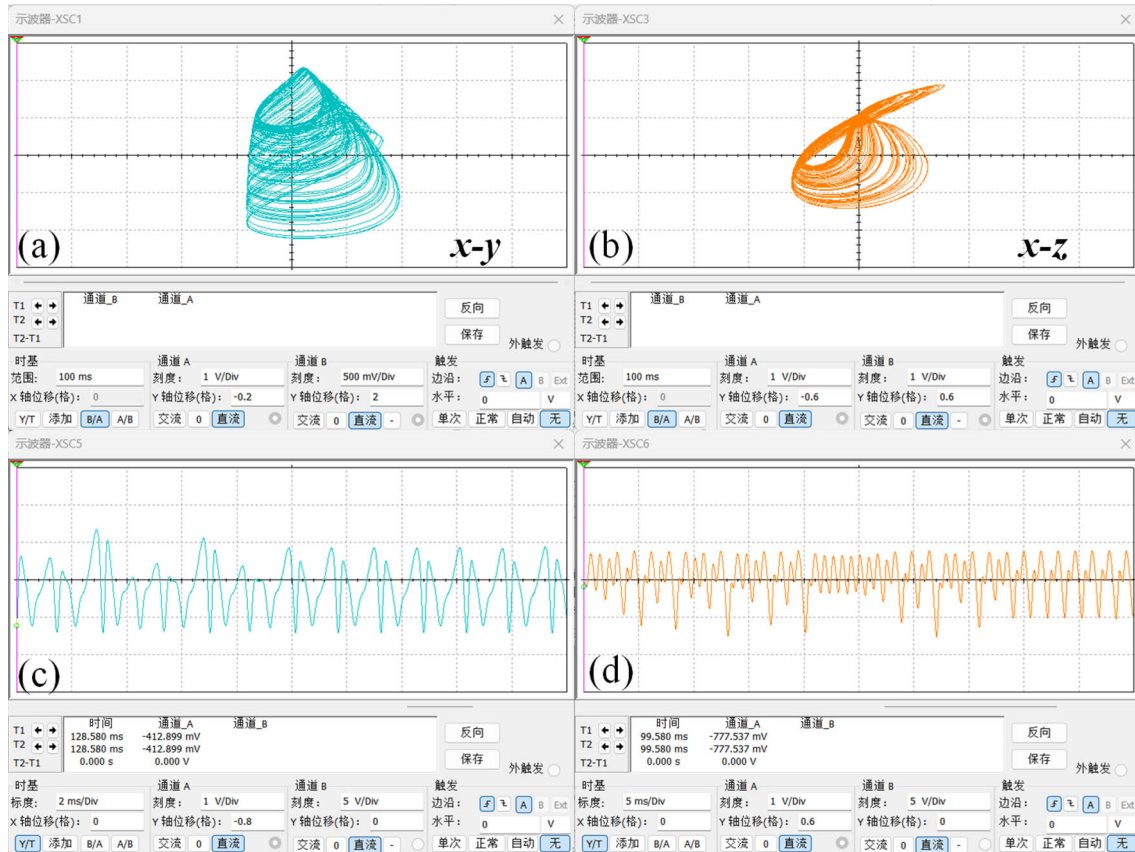
Circuit analysis is performed to obtain circuit Eq. (13):

$$\begin{cases} \dot{x} = \frac{V_2(V_1 - z)}{10R_1C_1}, \\ \dot{y} = -\frac{z^2}{R_2C_2} - \frac{y}{R_3C_2}, \\ \dot{z} = \frac{V_3(x - y)}{10R_4C_3}. \end{cases} \quad (13)$$

Here we set circuit parameters  $R_3 = R_4 = 10 \text{ k}\Omega$ ,  $R_4 = 2.5 \text{ k}\Omega$ ,  $R_2 = 325 \Omega$ , capacitors are all set to  $10 \text{ nF}$ ,  $V_1 = 0.25 \text{ V}$ ,  $V_2 = V_3 = 10 \text{ V}$ ,  $\text{VCC} = 18 \text{ V}$ ,  $\text{VEE} = -18 \text{ V}$ . The phase track diagram and waveform diagram generated by the circuit are shown in Fig. 24, and the results are consistent with those of the classical circuit under the condition of  $d_1 = d_2 = 0$ .

#### 4.2 Simplified circuit of system (11)

The simplified circuit of system (11) is shown in Fig. 25 below. Compared with the classical circuit, one multiplier is added, two operational amps and several resistors are reduced. For the equation  $\dot{x} = z^2 + y$ , the multiplier is used to form the quadratic term and the operational amplifier is used to form the integral circuit. For the equation  $\dot{y} = -bz$ , since there is only one term on the right side of the equation and it is not the inverse variable of  $y$ , if the multiplier and capacitor are introduced, additional terms need to be added, which makes the overall circuit more complicated, so the operational amplifier integral circuit is directly used; For the equation  $\dot{z} = -az + x + y$ , the parallel coupling of resistors and capacitors can be used to produce  $-az$  and the multiplier can be used to produce  $x - (y)$  to reduce the use of resistance and simplify the circuit.

**Fig. 25** Simplified circuit of system (11)**Fig. 26** Phase track diagram and waveform diagram of simplified circuit of system (11): **a** x-y plane, **b** x-z plane, **c** chaotic signal  $x(t)$ , **d** chaotic signal  $y(t)$ 

Circuit Eq. (14) can be obtained by similar circuit analysis:

$$\begin{cases} \dot{x} = \frac{z^2}{10R_5C_1} + \frac{y}{R_6C_1}, \\ \dot{y} = -\frac{z}{R_7C_2}, \\ \dot{z} = -\frac{z}{R_1C_3} + \frac{V_1(x+y)}{10R_2C_3}. \end{cases} \quad (14)$$

Here we set circuit parameters  $R_2 = R_6 = 10 \text{ k}\Omega$ ,  $R_7 = 25 \text{ k}\Omega$ ,  $R_3 = R_4 = 20 \text{ k}\Omega$ ,  $R_5 = 1 \text{ k}\Omega$ ,  $R_1 = 64 \text{ k}\Omega$ , capacitors are all set to  $10 \text{ nF}$ ,  $V_1 = 10 \text{ V}$ ,  $\text{VCC} = 18 \text{ V}$ ,  $\text{VEE} = -18 \text{ V}$ . The phase track diagram and waveform diagram generated by the circuit are shown in Fig. 26, and the results are consistent with those of the classical circuit under the condition of  $d_1 = d_2 = 0$ .

#### 4.3 Simplified circuit of system (12)

The simplified circuit of system (12) is shown in Fig. 27 below. Compared with the classical circuit, one multiplier is added, three operational amps and several resistors are reduced. For the equation  $\dot{x} = -ay$ , the simplified method of the third equation of system (11) is the same as that of directly using the integral circuit; For the equation  $\dot{y} = x + z$ , the multiplier is used to realize  $x(-z)$ , and

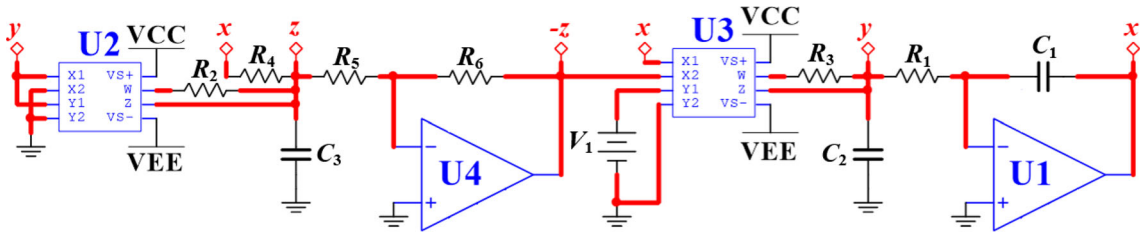


**Fig. 27** Simplified circuit of system (12)

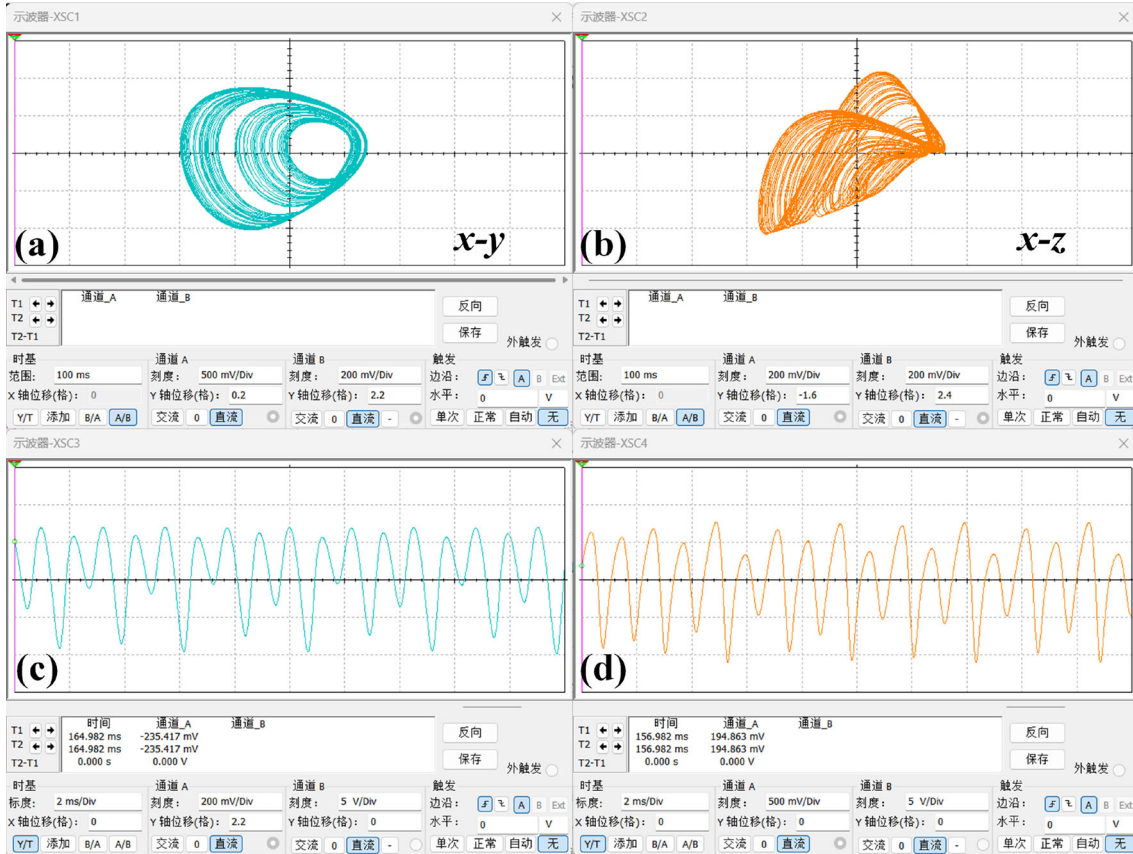


**Fig. 28** Phase track diagram and waveform diagram of simplified circuit of system (12): **a**  $x$ - $y$  plane, **b**  $x$ - $z$  plane, **c** chaotic signal  $x(t)$ , **d** chaotic signal  $y(t)$

then connect the capacitor to realize the integration; For the equation  $\dot{z} = x - z + y^2$ , the multiplier is used to achieve the quadratic term  $y^2$ , using the resistance capacitance series coupling method to achieve  $x$ - $z$ .

The circuit system Eq. (15) is obtained by the similar analysis:

$$\begin{cases} \dot{x} = -\frac{y}{R_1 C_1}, \\ \dot{y} = \frac{V_1(x+z)}{10R_3 C_2}, \\ \dot{z} = \frac{x-z}{R_4 C_3} + \frac{y^2}{10R_2 C_3}. \end{cases} \quad (15)$$

The circuit element paraments are selected as follows:  $R_5 = R_6 = 20 \text{ k}\Omega$ ,  $R_3 = R_4 = 1 \text{ k}\Omega$ ,  $R_2 = 100 \Omega$ ,  $R_1 = 25 \text{ k}\Omega$ ,  $C_1 = 20 \text{ nF}$ ,  $C_2 = C_3 = 100 \text{ nF}$ ,  $V_1 = 10 \text{ V}$ ,  $\text{VCC} = 15 \text{ V}$ ,  $\text{VEE} = -15 \text{ V}$ . The phase track diagram and waveform diagram generated by the circuit are shown in Fig. 28, and the results are consistent with those of the classical circuit under the condition of  $d_1 = d_2 = 0$ .

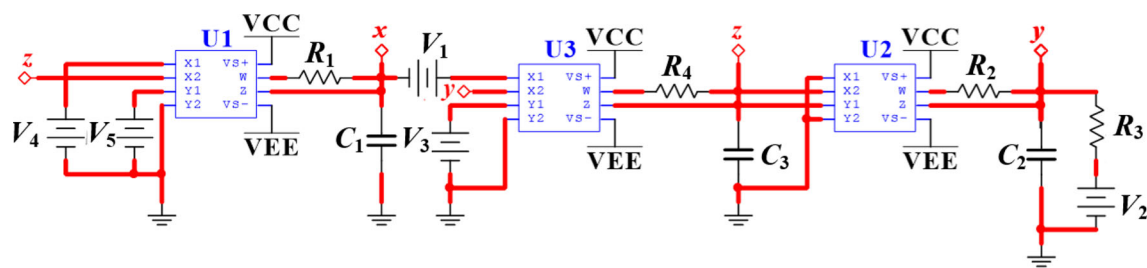


**Fig. 29** The simplified circuit that enables system (1) offset boosting

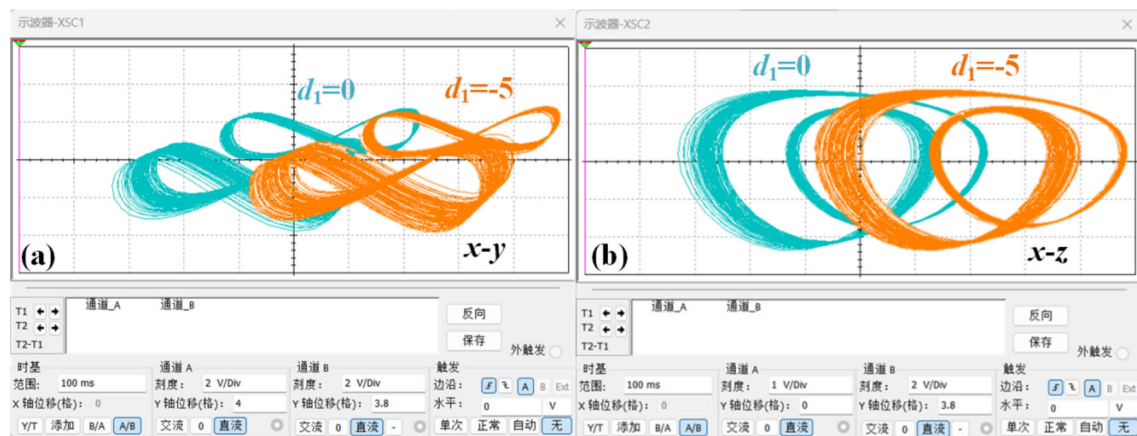


**Fig. 30** Single offset boosting control in system (1) with  $d_2 = 0$ : **a**  $x-y$ , **b**  $x-z$ . Here  $d_1 = 0$ , IC =  $(-1, 0, 0)$  is blue,  $d_1 = -5$ , IC =  $(4, 0, 0)$  is orange

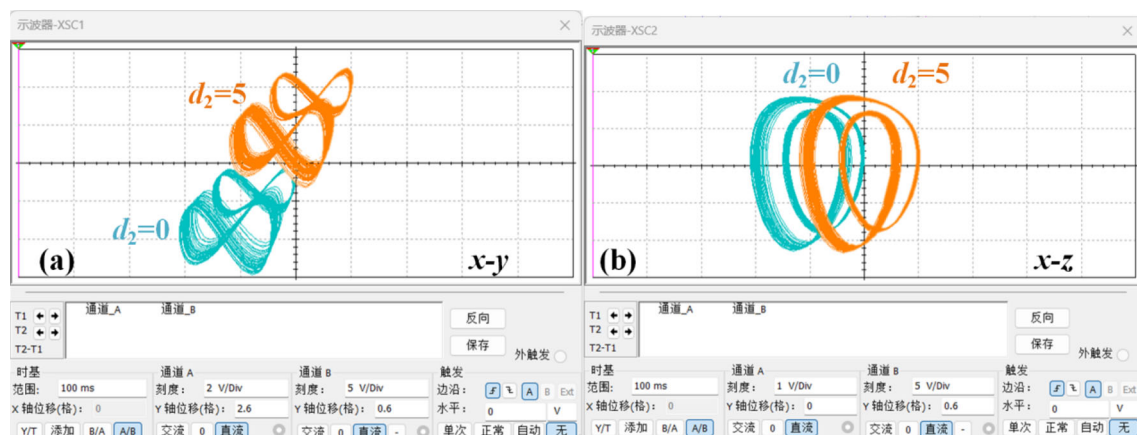


**Fig. 31** Common offset boosting control in system (1) with  $d_1 = 0$ : **a**  $x-y$ , **b**  $x-z$ . Here  $d_2 = 0$ , IC =  $(-1, 0, 0)$  is blue,  $d_2 = 5$ , IC =  $(4, 5, 0)$  is orange

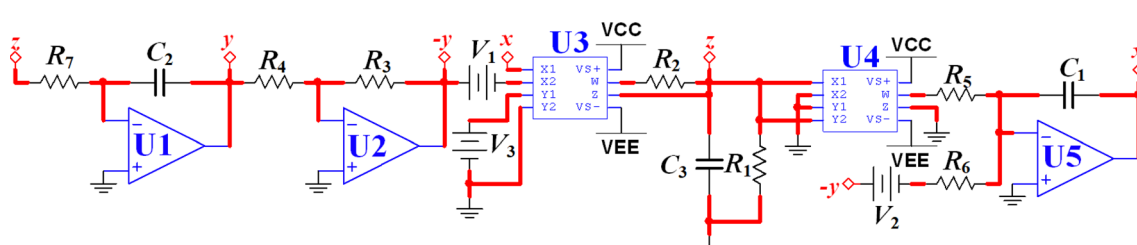


**Fig. 32** The simplified circuit that enables system (5) offset boosting

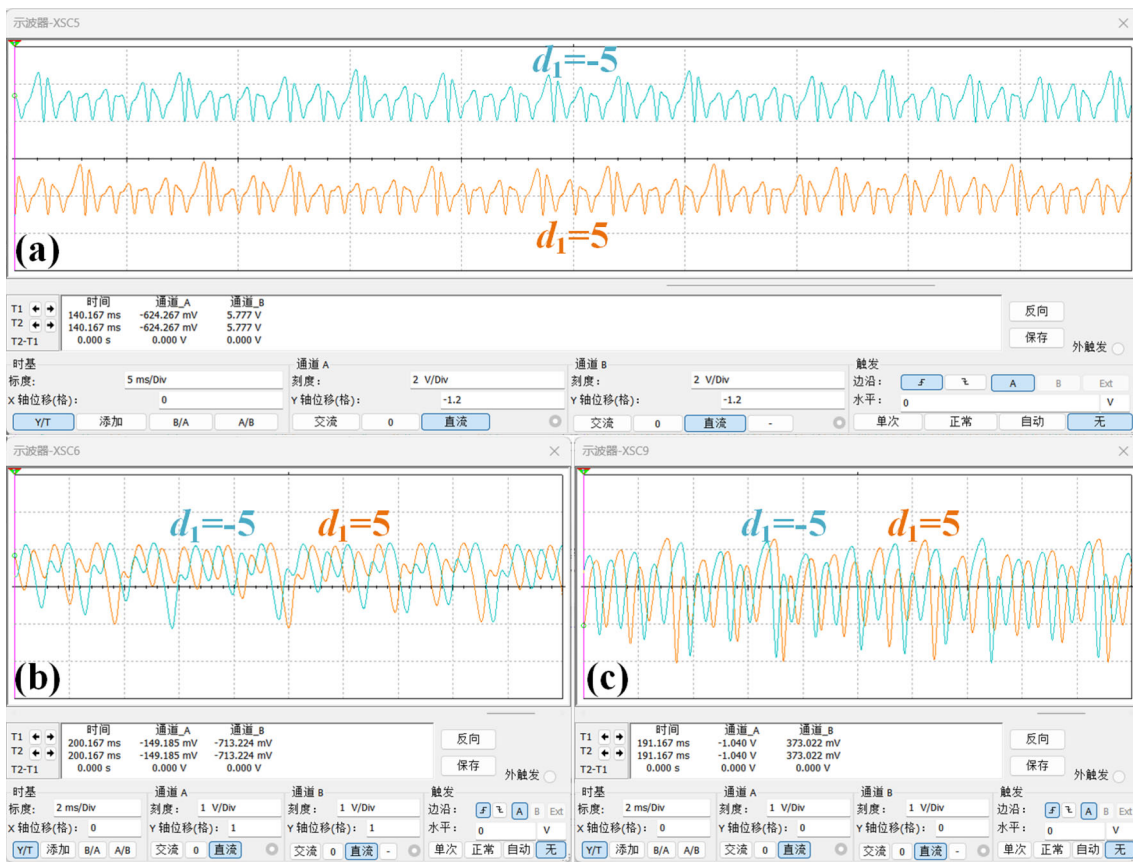


**Fig. 33** Single offset boosting control in system (5) with  $d_2 = 0$ : **a** chaotic signal  $x(t)$ , **b** chaotic signal  $y(t)$ , **c** chaotic signal  $z(t)$ . Here  $d_1 = 5$ , IC = (6, 1, 1) is blue,  $d_1 = 5$ , IC = (4, 1, 1) is orange

#### 4.4 Offset boosting in the simplified circuit

In the classical circuit, the DC power supply and resistance are used in series combined with the integral circuit method to achieve the constant  $d_1, d_2$  in the equation. Additional resistance will increase the cost and complexity of the circuit. To realize the bias control of the circuit while simplifying the circuit, the method of connecting the DC power supply in series is used to provide voltage at specific nodes of the circuit to achieve the bias control of the circuit.

For system (1), as shown in Fig. 29, we add DC power supply  $V_1$  and  $V_2$  based on Fig. 23 to achieve offset boosting of constant  $d_1$  and  $d_2$  equivalent.

According to the superposition theorem analysis, the circuit Eq. (16) can be obtained.

$$\begin{cases} \dot{x} = \frac{V_5}{10R_1C_1}(V_4 - z), \\ \dot{y} = -\frac{z^2}{10R_2C_2} + \frac{V_2 - y}{R_3C_2}, \\ \dot{z} = \frac{V_3}{10R_4C_3}(x - y + V_1). \end{cases} \quad (16)$$

Here, the circuit parameters are set to be consistent with circuit Eq. (13) except that  $R_2$  is modified to  $360 \Omega$ . As shown in Figs. 30, 31, the negative constant  $d_1$  causes the attractor to move in the positive direction of  $x$ , and the positive constant  $d_2$  causes the attractor to move in the positive direction of  $x$  and  $y$ , which is consistent with the results achieved by the classical circuit.

For system (5), we implement simplified offset boosting in the same way, as shown in Fig. 32.

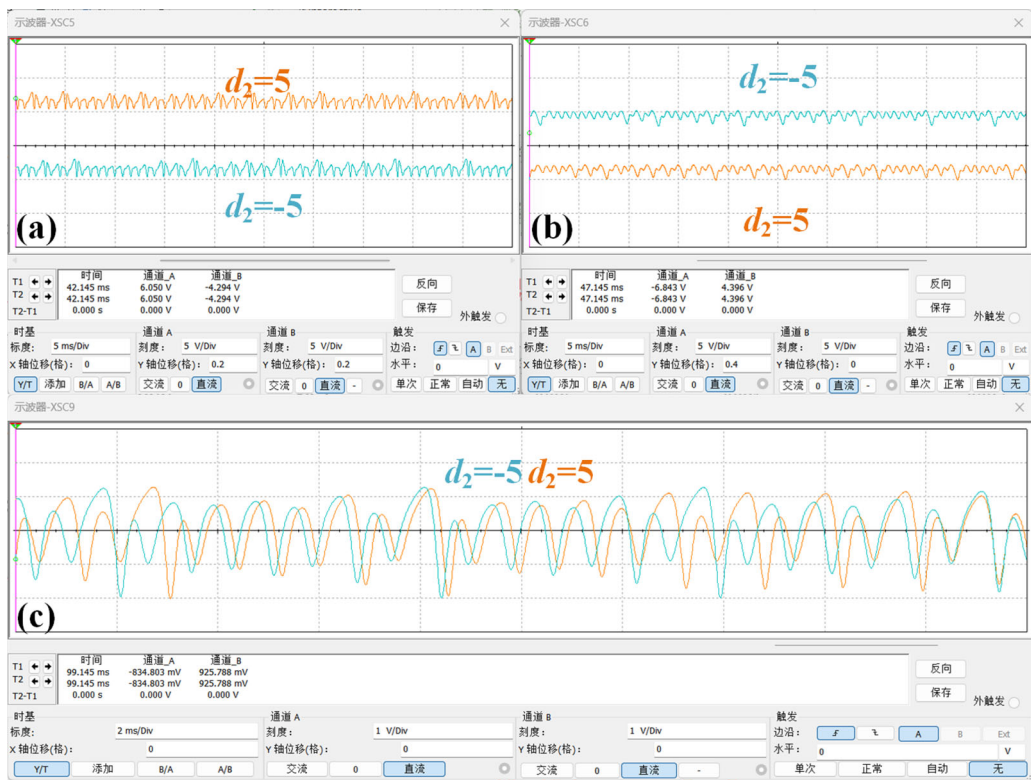


**Fig. 34** Reverse offset boosting control in system (5) with  $d_1 = 0$ : **a** chaotic signal  $x(t)$ , **b** chaotic signal  $y(t)$ , **c** chaotic signal  $z(t)$ . Here  $d_2 = -5$ , IC =  $(-4, 4, 1)$  is blue,  $d_2 = 5$ , IC =  $(6, -6, 1)$  is orange

Equation (17) can be obtained by similar circuit analysis:

$$\begin{cases} \dot{x} = \frac{z^2}{10R_5C_1} + \frac{y + V_2}{R_6C_1}, \\ \dot{y} = -\frac{z}{R_7C_2}, \\ \dot{z} = -\frac{z}{R_1C_3} + \frac{V_3(x + y + V_1)}{10R_2C_3}. \end{cases} \quad (17)$$

Here we set the circuit parameters to be consistent with the circuit Eq. (14). By observing the waveform changes, it is found that the normal number  $d_1$  causes the attractor to move in the negative direction of  $x$ , and the positive number  $d_2$  causes the attractor to move in the negative direction of  $x$  and the positive direction of  $y$ , as shown in Figs. 33, 34, and 35 can also prove this point.

For system (7), we implement simplified circuit of offset boosting in the same way, as shown in Fig. 36:

Equation (18) can be obtained by similar circuit analysis:

$$\begin{cases} \dot{x} = -\frac{y}{R_1C_1}, \\ \dot{y} = \frac{V_3(x + z + V_1)}{10R_3C_2}, \\ \dot{z} = \frac{x - z + V_2}{R_4C_3} + \frac{y^2}{10R_2C_3}. \end{cases} \quad (18)$$

Here we set the circuit parameters to be consistent with the circuit Eq. (15). As shown in Figs. 37 and 38, the negative constant  $d_1$  causes the attractor to move in the positive direction of  $x$ ; The negative constant  $d_2$  causes the attractor to move in the positive  $x$  direction and the negative  $z$  direction.

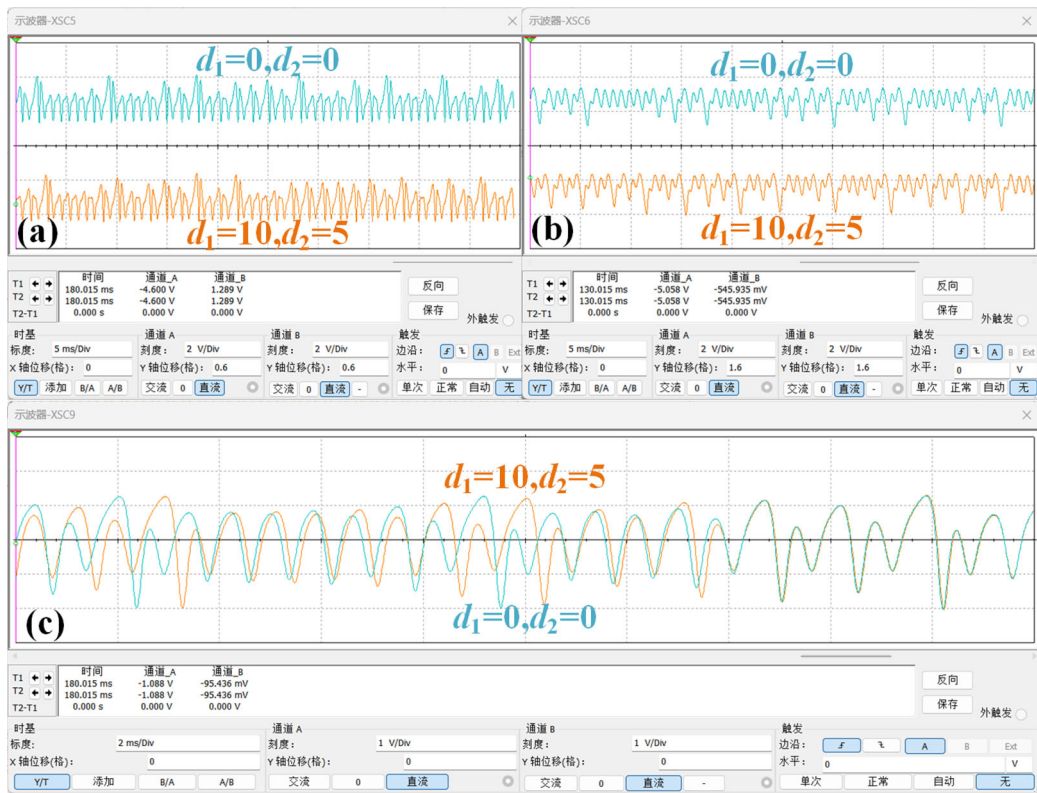


**Fig. 35** Differential offset boosting control of  $d_1$  and  $d_2$  in system (5): **a** chaotic signal  $x(t)$ , **b** chaotic signal  $y(t)$ , **c** chaotic signal  $z(t)$ . Here  $d_1, d_2 = 0$ , IC =  $(-1, 0, 0)$  is blue,  $d_1 = 10, d_2 = 5$ , IC =  $(-6, 5, 1)$  is orange

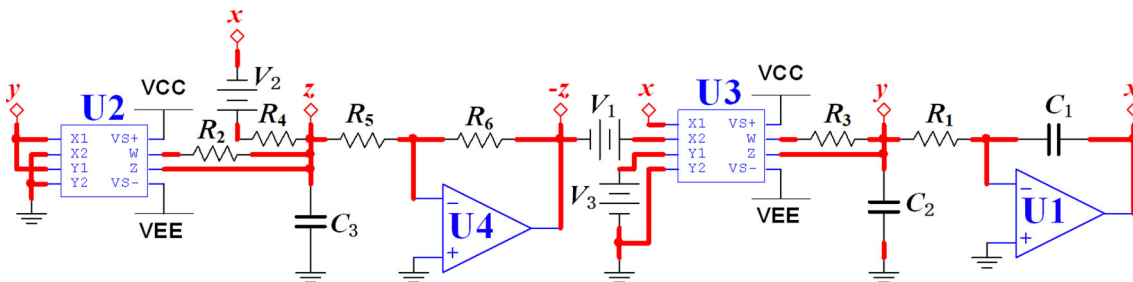


**Fig. 36** A simplified circuit that enables system (7) offset boosting

## 5 Implementation based on FPAA

Anadigm DualApex Development with two AN231E04 chips is used here to build the circuit to implement the system (1) under non-zero initial conditions. Since dpASP has a differential output voltage of  $\pm 3$  V, the system (1) needs to be amplitude-modulated so that the voltage is always within the signal range of  $\pm 3$  V. Scale system (1) as  $x \rightarrow 5x$ ,  $y \rightarrow 5y$ ,  $z \rightarrow 2z$ , as follows:

$$\begin{cases} \dot{x} = \frac{1}{5} - \frac{2az}{5}, \\ \dot{y} = \frac{-4bz^2}{5} - \frac{y}{5} + \frac{d_2}{5}, \\ \dot{z} = \frac{5x}{2} - \frac{5y}{2} + \frac{d_1}{2}. \end{cases} \quad (19)$$

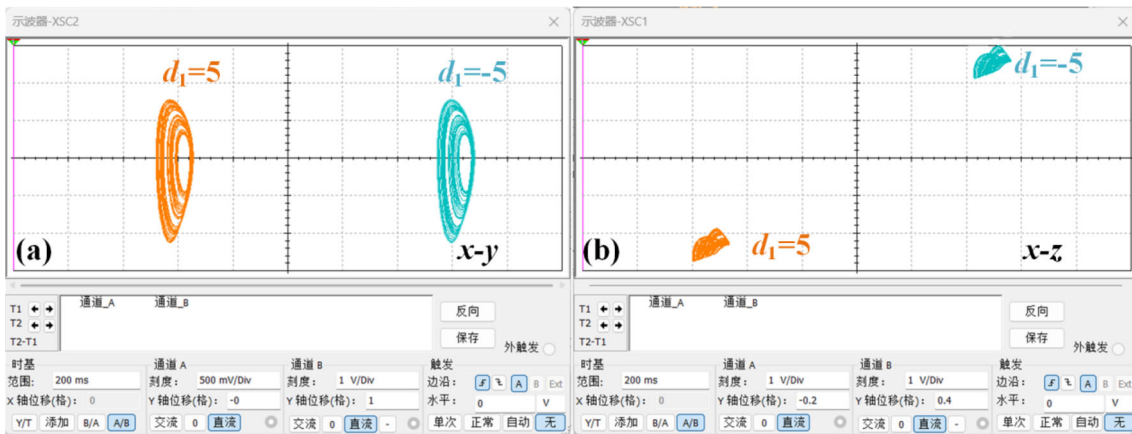


**Fig. 37** Common offset boosting control in system (7) with  $d_2 = 0$ : **a**  $x-y$ , **b**  $x-z$ . Here  $d_1 = -5$ , IC = (2.5, 0.3, 2.5) is blue,  $d_1 = 5$ , IC = (2.5, 0.3, 2.5) is orange

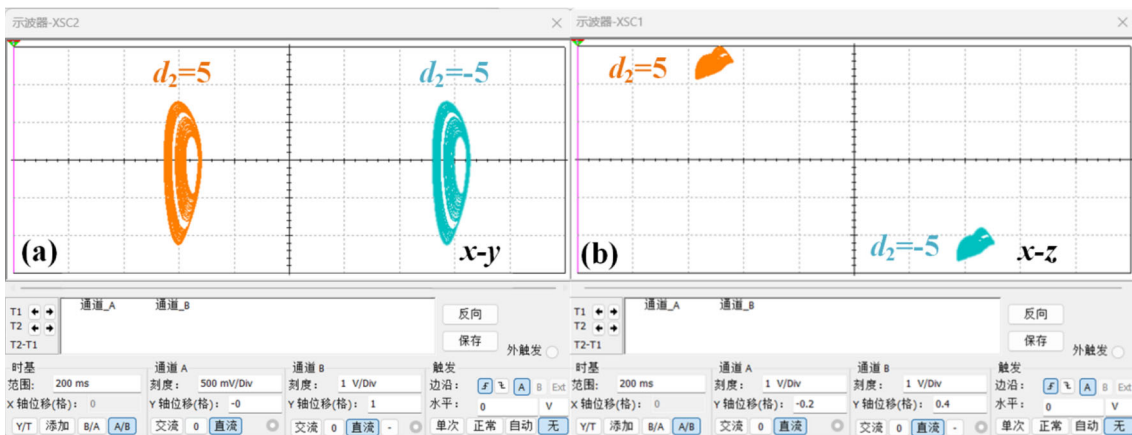


**Fig. 38** Reverse offset boosting control in system (7) with  $d_2 = 0$ : **a**  $x-y$  plane, **b**  $x-z$  plane. Here  $d_2 = -5$ , IC = (2.5, 0.3, 2.5) is blue,  $d_2 = 5$ , IC = (2.5, 0.3, 2.5) is orange

Since the initial value of system (1) is  $(4, 0, 0)$  when  $d_1 = -5$  and  $d_2 = 0$ , and then  $x$ ,  $y$ , and  $z$  are scaled, the initial value of system (1) in AnadigmDesigner2 should be  $(0.8, 0, 0)$ . According to the conventional setup, since the integrator is not charged, the initial value of the system is  $(0, 0, 0)$ , and system (1) cannot be implemented. To set the non-zero condition, the integrator needs to be charged before the development version runs the circuit. Because the resources in a single chip are insufficient, the system is built by two chips. The circuit schematic diagram is shown as systemA and systemB in Fig. 39 below. On this basis, the initial value of the circuit is set by constructing chips systemA\_ic and systemB\_ic. Through the dynamic configuration function of the chip, the main configuration AHF file of the chip systemA and systemB and the dynamic configuration AHF file of the chip systemA\_ic and systemB\_ic are downloaded to the development version in turn.

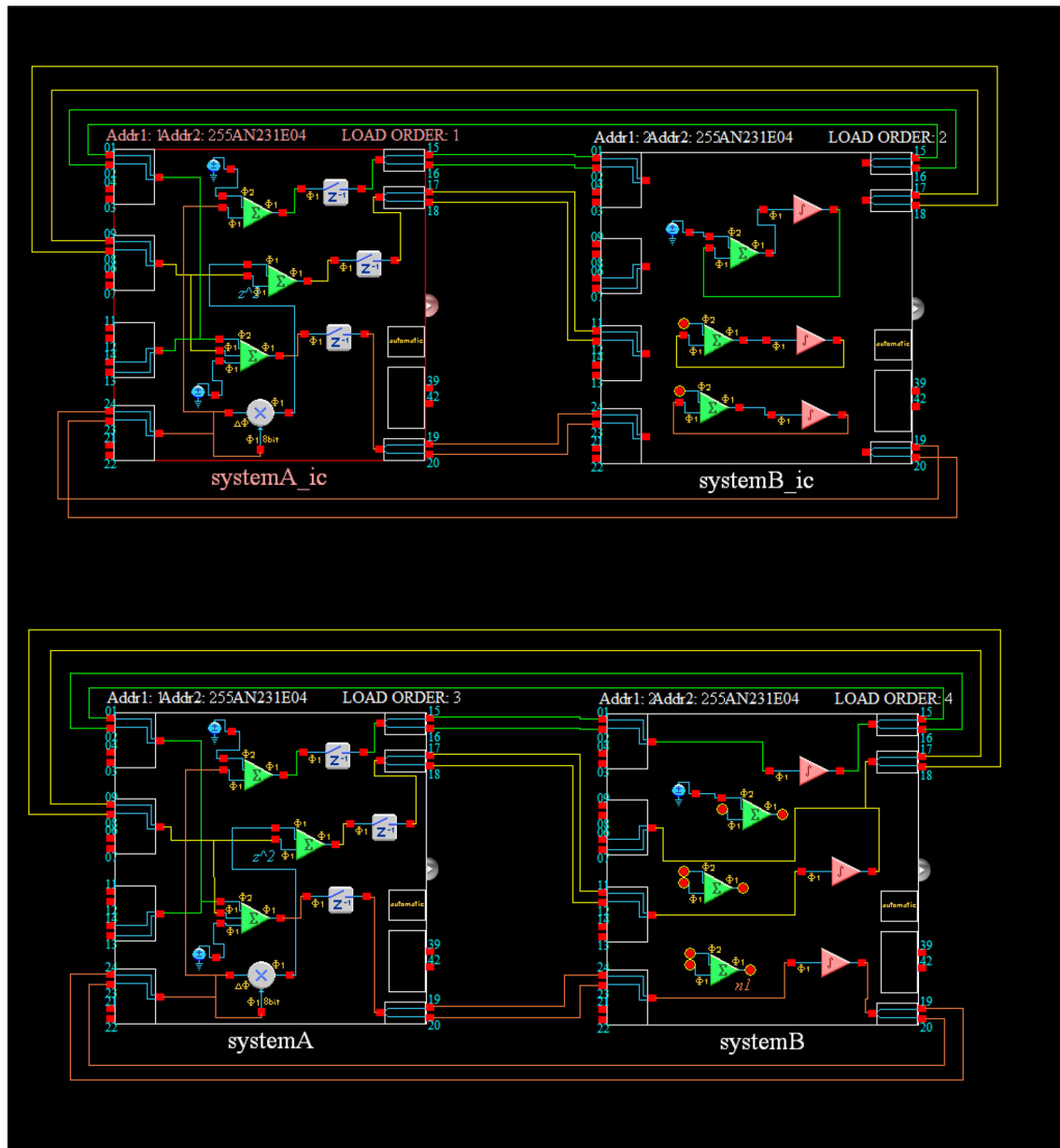


**Fig. 39** Circuit diagram of system (1) in AnadigmDesigne2 with the initial conditions (0.8, 0, 0)

For FPAA to output chaotic system (1), the Configurable Analog Modules of **systemA\_ic**, and **systemB\_ic** in Fig. 39 are set as shown in Table 2. The **systemA** and **systemB** parameters are the same as before. The hardware implementation platform of the entire system (1) and the output effect of the physical oscilloscope are all shown in Fig. 40.

**Table 2** CAM parameters of circuit in Fig. 33 for systemA\_ic and systemB\_ic

Name	Options	Parameters	Clocks
systemA_ic			
Multiplier	Sample and Off: Hold	Multiplication 1.00 Factor	ClockA:250 kHz ClockB:4 MHz
SumDiff	Output Phase: Phase 1 Input 1: Non-inverting Input 2: Inverting Input 3: Off Input 4: Off	Gain 1 0.1 Gain 2 1.56	ClockA:250 kHz
SumDiff	Output Phase: Phase 1 Input 1: Inverting Input 2: Inverting Input 3: Off Input 4: Off	Gain 1 2.80 Gain 2 1.00	ClockA:250 kHz
SumDiff	Output Phase: Phase 2 Input 1: Non-inverting Input 2: Inverting Input 3: Inverting Input 4: Off	Gain 1 2.50 Gain 2 2.50 Gain 3 1.25	ClockA:250 kHz
Voltage	Polarity positive (+ 2 V)		
Hold	Input Sampling Phase: Phase 1		ClockA:250 kHz
systemB_ic			
Integrator	Polarity: Non-inverting Input Sampling Phase: Phase 1 Compare Control To: No Reset	Integration Const:0.0025 [1/us]	ClockA:250 kHz
SumDiff	Output Phase: Phase 1 Input 1: Non-inverting Input 2: Inverting Input 3: Off Input 4: Off	Gain 1: 0.400 Gain 2: 1.00	ClockA:250 kHz
SumDiff	Output Phase: Phase 1 Input 1: Non-inverting Input 2: Inverting Input 3: Off Input 4: Off	Gain 1: 1.00 Gain 2: 1.00	ClockA:250 kHz
SumDiff	Output Phase: Phase 1 Input 1: Non-inverting Input 2: Inverting Input 3: Off Input 4: Off	Gain 1: 1.00 Gain 2: 1.00	ClockA:250 kHz
Voltage	Polarity positive (+ 2 V)		

## 6 Discussion and summary

Chaotic systems have found extensive applications across diverse fields, where offset boosting and amplitude control are crucial for chaotic signal conditioning and chaotic-based electronics engineering, particularly in the realm of chaotic radar systems. Two independent offset boosting controllers in chaotic system can meet the needs of multi-signal conditioning. In this paper, three kinds of two-dimensional offset boostable chaotic systems are realized by using the classical circuit based on the sum and integral circuit,

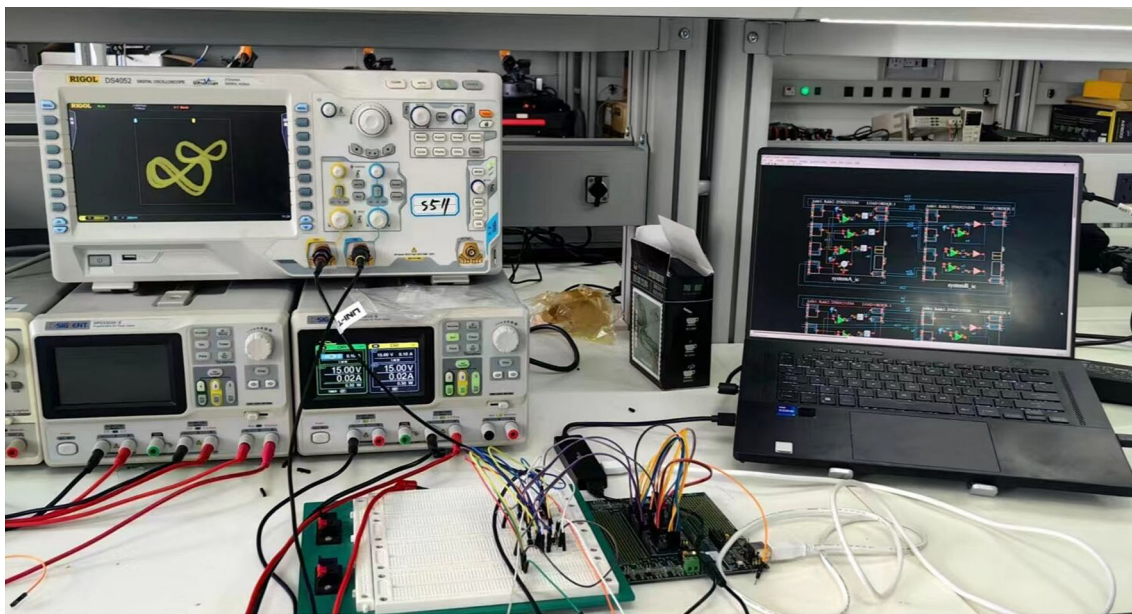


**Fig. 40** Hardware for showing phase orbits on physical oscilloscope

and the realizability of the two-dimensional offset boostable chaotic system is proved, the classical circuit is simplified, and the complexity of the circuit is reduced. On this basis, a method of simplifying the circuit to realize the offset boosting is proposed, the offset boosting is verified, and the application range of the simplification principle is extended. Finally, based on the platform of FPAAs, the systems are realized outputting corresponding chaotic signals. This verifies the feasibility of two-dimensional offset boosting and confirms the great convenience for chaotic signal conditioning.

**Acknowledgements** This work was supported by the Research and Innovation Training Projects of Dream Harvesting Space (DHS), and financially by the National Natural Science Foundation of China (Grant No.: 62371242).

**Data Availability Statement** No data associated in the manuscript.

## References

1. K.W. Tang, W.K.S. Tang, K.F. Man, A chaos-based pseudo-random number generator and its application in voice communications. *Int. J. Bifurc. Chaos* **17**(3), 923–933 (2007)
2. S. He, L. Fu, Y. Lu et al., Analog circuit of a simplified Tent map and its application in sensor position optimization. *IEEE Trans. Circuits Syst. II Express Briefs* **70**(3), 885–888 (2022)
3. Q. Lai, L. Yang, Y. Liu, Design and realization of discrete memristive hyperchaotic map with application in image encryption. *Chaos Solitons Fract.* **165**, 112781 (2022)
4. F. Aliabadi, M.H. Majidi, S. Khorashadizadeh, Chaos synchronization using adaptive quantum neural networks and its application in secure communication and cryptography. *Neural Comput. Appl.* **34**(8), 6521–6533 (2022)
5. H. Li, Z. Hua, H. Bao et al., Two-dimensional memristive hyperchaotic maps and application in secure communication. *IEEE Trans. Industr. Electron.* **68**(10), 9931–9940 (2020)
6. A. Durdu, Image transfer with secure communications application using a new reversible chaotic image encryption. *Multimed. Tools Appl.* **83**(2), 3397–3424 (2024)
7. H. Wen, Y. Lin, Cryptanalysis of an image encryption algorithm using quantum chaotic map and DNA coding. *Expert Syst. Appl.* **237**, 121514 (2024)
8. H. Wen, R. Chen, J. Yang et al., Security analysis of a color image encryption based on bit-level and chaotic map. *Multimed. Tools Appl.* **83**(2), 4133–4149 (2024)
9. Z. Chen, X. Wang, C. Yang et al., Memristive circuit design for personalized emotion generation with memory and retrieval functions. *IEEE Trans. Cognit. Dev. Syst.* (2023). <https://doi.org/10.1109/TCDS.2023.3317066>
10. J. Sun, Y. Zhai, P. Liu et al., Memristor-based neural network circuit of associative memory with overshadowing and emotion congruent effect. *IEEE Trans. Neural Netw. Learn. Syst.* (2024). <https://doi.org/10.1109/TNNLS.2023.3348553>
11. W. Yao, C. Wang, Y. Sun et al., Robust multimode function synchronization of memristive neural networks with parameter perturbations and time-varying delays. *IEEE Trans. Syst. Man Cybern. Syst.* **52**(1), 260–274 (2020)
12. X. Yang, W. Wang, Chaotic signal denoising based on energy selection TQWT and adaptive SVD. *Sci. Rep.* **13**(1), 18873 (2023)
13. Z. Liu, X. Zhu, W. Hu et al., Principles of chaotic signal radar. *Int. J. Bifurc. Chaos* **17**(5), 1735–1739 (2007)
14. B. Yang, J.S. Sun, H. Chi et al., Joint radar and communication system based on a chaotic optoelectronic oscillator. *Opt. Commun.* **554**, 130123 (2024)
15. F.Y. Lin, J.M. Liu, Ambiguity functions of laser-based chaotic radar. *IEEE J. Quantum Electron.* **40**(12), 1732–1738 (2004)
16. C. Li, J.C. Sprott, Amplitude control approach for chaotic signals. *Nonlinear Dyn.* **73**, 1335–1341 (2013)
17. C. Li, J.C. Sprott, Variable-boostable chaotic flows. *Optik* **127**(22), 10389–10398 (2016)

18. Q. Wu, Q. Hong, X. Liu et al., A novel amplitude control method for constructing nested hidden multi-butterfly and multiscroll chaotic attractors. *Chaos Solitons Fract.* **134**, 109727 (2020)
19. X. Zhang, C. Li, X. Gao et al., Reproducing countless hidden attractors in a memristive system based on offset boosting. *Eur. Phys. J. Plus* **139**(2), 1–11 (2024)
20. C. Li, T. Lei, X. Wang et al., Dynamics editing based on offset boosting. *Chaos Interdiscip. J. Nonlinear Sci.* **30**(6), 063124 (2020)
21. C. Li, Y. Gao, T. Lei et al., Two independent offset controllers in a three-dimensional chaotic system. *Int. J. Bifurc. Chaos* **34**(1), 2450008 (2024)
22. X. Zhang, C. Li, K. Huang et al., A chaotic oscillator with three independent offset boosters and its simplified circuit implementation. *IEEE Trans. Circuits Syst. II Express Briefs* **71**(1), 51–55 (2024)
23. F. Min, W. Zhang, Z. Ji et al., Switching dynamics of a non-autonomous FitzHugh-Nagumo circuit with piecewise-linear flux-controlled memristor. *Chaos Solitons Fract.* **152**, 111369 (2021)
24. X. Zhang, C. Li, L. Minati et al., Offset-dominated uncountably many hyperchaotic oscillations. *IEEE Trans. Industr. Inf.* **20**(5), 7936–7946 (2024)
25. C. Chen, F. Min, ReLU-type memristor-based Hopfield neural network. *Eur. Phys. J. Spec. Top.* **231**(16), 2979–2992 (2022)
26. Y. Gao, C. Li, I. Moroz et al., Approximate equivalence of higher-order feedback and its application in chaotic systems. *Int. J. Bifurc. Chaos* **34**(1), 2450007 (2024)
27. X. Zhang, J. Liu, D. Wang et al., Geometric control and synchronization of a complex-valued laser chain network. *Nonlinear Dyn.* **111**(7), 6395–6410 (2023)
28. Y. Li, C. Li, S. Zhang et al., A self-reproduction hyperchaotic map with compound lattice dynamics. *IEEE Trans. Industr. Electron.* **69**(10), 10564–10572 (2022)
29. T. Ma, J. Mou, H. Yan et al., A new class of Hopfield neural network with double memristive synapses and its DSP implementation. *Eur. Phys. J. Plus* **137**(10), 1–19 (2022)
30. J.N. Blakely, M.B. Eskridge, N.J. Corron, A simple Lorenz circuit and its radio frequency implementation. *Chaos Interdiscip. J. Nonlinear Sci.* **17**(2) (2007)
31. J. Wu, C. Li, X. Ma et al., Simplification of chaotic circuits with quadratic nonlinearity. *IEEE Trans. Circuits Syst. II Express Briefs* **69**(3), 1837–1841 (2021)
32. C. Li, W.J.C. Thio, J.C. Sprott et al., Constructing infinitely many attractors in a programmable chaotic circuit. *IEEE Access*. **6**, 29003–29012 (2018)

Springer Nature or its licensor (e.g. a society or other partner) holds exclusive rights to this article under a publishing agreement with the author(s) or other rightsholder(s); author self-archiving of the accepted manuscript version of this article is solely governed by the terms of such publishing agreement and applicable law.